TURKISH REPUBLIC
MARMARA UNIVERSITY
INSTITUTE OF HEALTH SCIENCES

EFFECT OF *EREMURUS SPECTABILIS* EXTRACT ON HEP3B CELL LINE

NOUR ALHALAK

MASTERS THESIS

SUPERVISOR

ASSIST. PROF. TURGUT ŞEKERLER

BIOCHEMISTRY (PHARMACY) MASTER'S DEGREE PROGRAM

ISTANBUL- 2025

TURKISH REPUBLIC
MARMARA UNIVERSITY
INSTITUTE OF HEALTH SCIENCES

EFFECT OF *EREMURUS SPECTABILIS* EXTRACT ON HEP3B CELL LINE

NOUR ALHALAK

MASTERS THESIS

SUPERVISOR

ASSIST. PROF. TURGUT ŞEKERLER

BIOCHEMISTRY (PHARMACY) MASTER'S DEGREE PROGRAM

ISTANBUL- 2025

STATEMENT

I hereby declare that this thesis study is my own work and that I have not engaged in any unethical behavior during the planning or writing of the thesis. I have sourced all the information in this thesis in compliance with academic and ethical guidelines. I have cited all information and comments not obtained through this thesis study, and the list of references includes these sources. Additionally, I hereby declare that I have not infringed on any patents or copyrights during the study and writing of this thesis.

NOUR ALHALAK

ACKNOWLEDGMENT

‘And He found you lost and guided you’ (Quran 93:7). With this profound guidance, I am eternally grateful to God for embracing me with His blessings throughout this journey.

As I conclude my research, I would like to take this opportunity to express my heartfelt gratitude to everyone who has played a significant role in my academic and personal journey. Their unwavering support and encouragement have been vital to my achievements, and I am sincerely grateful to each of them.

First and foremost, I want to express my deepest thanks to my beloved father, **Mohammad Alhalak**, for always being my unwavering support. Every step I’ve taken and everything I’ve achieved is a reflection of your unshakable belief in me, your boundless love, and your constant trust. Every success I celebrate is not just mine, but a tribute to the incredible father you’ve been, shaping me into who I am today. To my dearest mother, **Hanady Shboul**, my butterfly—I wish you were here to hold me and tell me you are proud. Words will never be enough to express how grateful I am for everything you’ve given me. I can only hope you are watching from above, knowing that I’ve done my best to make you proud.

A huge love and thanks to my sisters, Aya, Sara, Ghina, and Layan, for always being there. Your love and those countless video calls filled with laughter made even the loneliest moments feel warm. To my dear nephew, Ajouka Senior—thank you for arriving at just the *perfect* moment and shaking things up! While your timing might have delayed my thesis submission, you’ve also been a much-needed burst of joy and laughter in the middle of all the chaos, making every moment of waiting for your arrival worth it.

My amazing friends—Deema, Fatima, Asmaa, Aya, and Dania—thank you for your unconditional love and for being my constant source of positivity. You made it easier to face every challenge with a smile. A special heartfelt thanks to my Turkish friend, Rümeysa, whose support for me during the writing phase of my thesis meant so much. Your kindness and encouragement truly kept me going.

I would also like to express my sincere gratitude to my supervisor, **Dr. Turgut Şekerler**, for his continuous support, guidance, and unwavering belief in me. His kind words always touched my heart and motivated me to work even harder. I also want to thank **Dr. Farah Al-Mamoori** for her guidance and mentorship throughout my academic journey. I am deeply grateful for her patience in answering my many questions, always with a kind and generous heart.

A special thanks to the **Turkish Government Scholarship** for allowing me to pursue my dream of studying for a master's degree and conducting cancer research.

Lastly, and forever, I want to thank just Nour, who held my hand until the very end, lighting my path throughout this journey of studying abroad. I want to express my immense love for her for achieving one of her dreams and for staying strong no matter what.

This work was supported by the Research Fund of the University of Marmara (TYL-2024-11233).

CONTENTS

ABBREVIATIONS and SYMBOLS LIST i
FIGURES LIST iv
TABLES LIST vii
1. ÖZET 1
2. SUMMARY 2
3. INTRODUCTION and OBJECTIVE 3
4. BACKGROUND 6
4.1. Cancer 6
4.2. Carcinogenesis 6
4.2.1. DNA damage in carcinogenesis 7
4.3. Hepatocellular Carcinoma (HCC) 8
4.3.1. HCC etiology 9
4.3.2. HCC diagnostic approaches 12
4.3.3. HCC stages 14
4.3.4. HCC treatment approaches 15
4.4. Angiogenesis 18
4.4.1. Key stages of angiogenesis 19
4.4.2. Angiogenesis in pathological processes 20
4.4.3. Tumor angiogenesis and metastasis 20
4.4.4. Angiogenesis in hepatocellular carcinoma (HCC) 21
4.4.5. Mechanisms and inhibition of angiogenesis in HCC 21
4.4.6. Role of VEGF in angiogenesis 22
4.4.7. Anti-angiogenesis therapies in HCC 23
4.5. Drug Resistance in Hepatocellular Carcinoma 23
4.6. Eremurus spectabilis 25
4.6.1. Previous studies on anticancer effects of *E. spectabilis* 26
4.6.2. Nutritional, antioxidant, and antimicrobial properties of *E. spectabilis* .. 27

4.6.3. Therapeutic activities of *E. spectabilis* 28
4.6.4. Bioactive compounds isolated from *E. spectabilis* 28
5. MATERIALS and METHODS 29
5.1. Materials 29
5.2. Extraction Process 30
5.3. Hep3B Cell Culture and Handling Procedures 30
5.3.1 Cell thawing 30
5.3.2. Cell passaging 31
5.3.3. Cell counting 31
5.3.4. Cell freeze 32
5.4. Cell Viability Assay with Xcelligence® RTCA Assay 32
5.5. The Chick Embryo Chorioallantoic Membrane (CAM) Assay 34
5.4. Docking 38
5.5. Statistical Analysis 43
6. RESULTS 44
6.1. Cytotoxicity of *E. spectabilis* Fractions on Hep3B Cells 44
6.2. Anti-Angiogenic Activity of *E. spectabilis* Fractions 47
6.3. Molecular Docking Results 50
7. DISCUSSION and CONCLUSION 55
8. REFERENCES 58

ABBREVIATIONS and SYMBOLS LIST

A-549: Human alveolar adenocarcinoma

AFP: Alpha-fetoprotein

ALA: Alanine

ALKS: Activin receptor-like kinase

ALT: Alanine aminotransferase

Ang2: Angiopoietin-2

AST: Aspartate aminotransferase

AXIN1: Axis inhibitor-1

bFGF: Basic fibroblast growth factor

CaCo-2: Colon carcinoma cell line

CAM: Chorioallantoic membrane

CCN: Cellular communication network factor.

CD105: Cluster of differentiation 105

CEUS: Contrast-enhanced ultrasound

COX2: Cyclooxygenase-2

CT: Computed tomography

CYS: Cysteine

DMSO: Dimethyl sulfoxide

EC: Endothelial cell

ECM: Extracellular matrix

EDD: Embryonic day of development

ECOG: Eastern Cooperative Oncology Group

ES: *Eremurus spectabilis*

ESC: *Eremurus spectabilis* chloroform fraction

ESH: *Eremurus spectabilis* hexane fraction

ESAE: *Eremurus spectabilis* aqueous ethanol fraction

ESEA: *Eremurus spectabilis* ethyl acetate fraction

FBS: Fetal bovine serum

FGF2: Fibroblast growth factor 2

GLU: Glutamate

GLY: Glycine

HCC: Hepatocellular carcinoma

HBV: Hepatitis B virus

HCV: Hepatitis C virus

HEK293: Human embryonic kidney cells

Hep3B: Human hepatocellular carcinoma cell line

IC_{50}: Half-maximal inhibitory concentration

INR: International normalized ratio

LEU: Leucine

MRI: Magnetic resonance imaging

mPANC96: Human pancreatic adenocarcinoma

NAFLD: Non-alcoholic fatty liver disease

NCDDG: National Cooperative Drug Development Group

Ob-R: Leptin receptor

PDB: Protein Data Bank

PBS: Phosphate-buffered saline

PDGFR: Platelet-derived growth factor receptor

PGE2: Prostaglandin E2

PHE: Phenylalanine

PS: Performance Scale

RAF: Rapidly accelerated fibrosarcoma kinase

RNA: Ribonucleic acid

RCT: Randomized controlled trial

RTCA: Real-time cell analysis

SOX4: SRY-box transcription factor 4

TACE: Transarterial chemoembolization

TARE: Transarterial radioembolization

TERT: Telomerase reverse transcriptase

THR: Threonine

TP53: Tumor protein p53

TRC105: Anti-CD105 monoclonal antibody

U87MG: Glioblastoma cell line

US: Ultrasonography

VAL: Valine

VEGF: Vascular endothelial growth factor

Y-90: Yttrium-90

FIGURES LIST

Figure 1. Illustration of DNA damage and its progression to cancer if repair mechanisms fail……7

Figure 2. Progression of hepatocellular carcinoma (HCC)…….9

Figure 3. Angiogenesis…….19

Figure 4. Steps in angiogenesis……..20

Figure 5. Mechanisms of pro-angiogenic factors inducing angiogenesis and new potential targets inhibiting angiogenesis in HCC…….....22

Figure 6. *Eremurus spectabilis*……26

Figure 7. Chemical structures of compounds isolated from *E. spectabilis*……..28

Figure 8. Thoma slide used for cell counting external and microscopic views…….32

Figure 9. illustration of the methodology……..34

Figure 10. A schematic illustration of the chick chorioallantoic membrane (CAM) and the general structure of a five-day-old chick embryo in the egg……..35

Figure 11. Monitoring embryo viability…….36

Figure 12. Removal of 3 mL of albumin from eggs on embryonic day 3 (EDD3)……37

Figure 13. Circular opening (1-2 cm in diameter) created on the tops of eggs on embryonic day 4 (EDD4)…….37

Figure 14. Fractions were applied to the CAM layer on EDD6 using 6 mm sterile filter paper discs…….38

Figure 15. Downloading VEGFR2 (PDB ID: 2OH4) structure from the Protein Data Bank…….....39

Figure 16. Docking Preparation: VEGFR2 protein structure was prepared using the Dock Prep tool in Chimera……...40

Figure 17. Structure Minimization step……41

Figure 18. Grid Map Determination on VEGFR2 (2OH4)……42

Figure 19. Docking stimulation Using AutoDock Vina……43

Figure 20. The effect of ESH fraction treated with different concentrations at various time intervals on Hep3B cells……45

Figure 21. The effect of ESC fraction treated with different concentrations at various time intervals on Hep3B cells……45

Figure 22. The effect of ESEA fraction treated with different concentrations at various time intervals on Hep3B cells…….....46

Figure 23. The effect of ESAE fraction treated with different concentrations at various time intervals on Hep3B cells……46

Figure 24. The fold change in total vessel area for each ES fraction after 24 hours. 1: ESH, 2: ESC, 3: ESEA, and 4: ESAE……47

Figure 25. The fold change in branching points number for each ES fraction after 24 hours. 1: ESH, 2: ESC, 3: ESEA, and 4: ESAE……48

Figure 26. The fold change in total vessel length for each ES fraction after 24 hours. 1: ESH, 2: ESC, 3: ESEA, and 4: ESAE…….....48

Figure 27. Inhibition of the capillaries on the CAM by ES fractions 1: ESH, 2: ESC, 3: ESEA, and 4: ESAE in both Ic_{50} and $Ic_{50/2}$ doses compared to control after 24 hours……49

Figure 28. Illustration of capillary inhibition on the CAM by the ESC fraction at IC_{50} and $IC_{50/2}$ doses compared to the control after 24 hours……49

Figure 29. The binding pose of 7,10′-bichrysophanol with VEGF-2, displaying a binding energy of -10.8 kcal/mol……51

Figure 30. The binding pose of chrysalodin with VEGF-2, displaying a binding energy of -10.7 kcal/mol……51

Figure 31. 7,10′-Bichrysophanol–VEGF-2 binding (-10.8 kcal/mol)……. 52

Figure 32. Chrysaoldin–VEGF-2 binding (-10.7 kcal/mol)…….……53

TABLES LIST

Table 1. Docking Results: Binding Scores, Hydrogen Bonds, and Hydrophobic Interactions Number of Various ES Compounds (Control compounds *)……50

Table 2. Assessment of hydrophobic bonds between VEGF-2 and 7,10′bichrysophanol....52

Table 3. Assessment of hydrogen bonds between VEGF-2 and 7,10′bichrysophanol.....53

Table 4. Assessment of hydrophobic bonds between VEGF-2 and chrysalodin…….....54

Table 5. Assessment of hydrogen bonds between VEGF-2 and chrysalodin……54

1. ÖZET

Tez Başlığı: *Eremurus Spectabilis* Ekstresinin Hep3b Hücre Hattı Üzerindeki Etkisi.
Öğrenci Adı, Soyadı: Nour ALHALAK
Tez Danışmanı: Assist. Prof. Turgut ŞEKERLER
Program Adı: Biyokimya (Eczacılık) Yüksek Lisans Programı

Amaç: Hepatoselüler karsinom (HCC), ilerleyişinde anjiyogenezisin önemli ve hayati bir rol oynadığı, ciddi bir sağlık sorunudur. Günümüze kadar, tıbbi bitkiler, etkili antikanser ajanlar olarak hizmet edebilecek doğal bileşiklerin değerli bir kaynağı olmaya devam etmektedir. Geleneksel halk tıbbında kullanılan *Eremurus spectabilis* (ES), antikanser aktivitesi tam olarak belirlenmemiş bitkilerden biridir. Bu araştırmanın amacı, *E. spectabilis*'in farklı fraksiyonlarının Hep3B hücre hattı üzerindeki sitotoksik etkilerini ve anti-anjiogenik etkilerini araştırmaktır.
Gereç ve Yöntemler: Bitki fraksiyonlarının sitotoksisite deneyleri, Hep3B hücre hatlarında Xcelligence Gerçek Zamanlı Hücre Analizörü yöntemiyle araştırılmıştır. Fraksiyonların anti-anjiyogenez potansiyeli CAM testi ile incelenmiş ve anti-anjiyogenez mekanizmasını öngörmek için docking çalışmaları yapılmıştır.
Bulgular: Tüm ES fraksiyonlarının Hep3B'ye karşı anlamlı antikanser etkiler gösterdiği ortaya konulmuş olup, ESEA (24 saat IC50: 6,53 µg/mL) ve ESAE (24 saat IC50: 7,89 µg/mL) daha etkili bulunmuştur. Ayrıca, ESC fraksiyonu, toplam damar alanını, damar uzunluğunu ve dallanma noktalarını azaltarak güçlü bir anti-anjiyojenik aktivite sergilemiştir. Moleküler docking çalışmaları bu bulguları desteklemiştir. Test edilen *E. spectabilis* fitokimyasallarının hemen hemen tümü, özellikle -10.8 kcal/mol bağlanma skoruna ulaşan 7,10′-bikrizofanol, VEGFR-2 ile anlamlı ve güçlü etkileşimler göstermiştir.
Sonuç: Etkin bileşenleri belirlemek ve etki mekanizmalarını açıklamak için daha fazla araştırmaya ihtiyaç duyulmasına rağmen, bu sonuçlar E. spectabilis'i kanser tedavisi için çift etkili bir seçenek olarak önermektedir.

Anahtar Kelimeler: *Eremurus spectabilis*, hepatoselüler karsinom, sitotoksisite, anti-anjiyojenik, moleküler docking

2. SUMMARY

Thesis Title: Effect Of *Eremurus Spectabilis* Extract On Hep3b Cell Line
Student Name, Surname: Nour ALHALAK
Supervisor Name: Assist. Prof. Turgut ŞEKERLER
Program Name: Biochemistry (Pharmacy) Master's Program

Objective: Hepatocellular carcinoma (HCC) is a major health concern, with angiogenesis playing an important, vital role in its progression. Until our days, medicinal plants continue to be a valued source of natural compounds that have the potential to serve as effective anticancer agents. *Eremurus spectabilis* (ES), which has been used in traditional folk medicine, is one of the plants that has not been fully identified for its anticancer activity. The aim of this research is to investigate the cytotoxic effects of different fractions of *E. spectabilis* on the Hep3B cell line and their anti-angiogenic effects.
Materials and Methods: Plant fractions were investigated by the Xcelligence Real-Time Cell Analyzer method for cytotoxicity experiments on Hep3B cell lines. The anti-angiogenesis potential of the fractions was investigated using the CAM assay, and docking studies were conducted to predict the anti-angiogenesis mechanism.
Results: Significant anticancer effects against Hep3B were revealed by all ES fractions, with ESEA (24-hour IC50: 6.53 µg/mL) and ESAE (24-hour IC50: 7.89 µg/mL) being more effective. Moreover, the ESC fraction displayed a strong antiangiogenic activity by reducing the total vessel area, the vessel length, and the branching points. Molecular docking studies corroborated these findings. Almost all of the tested *E. spectabilis* phytochemicals exhibit significant and strong interactions with VEGFR-2, particularly 7,10′-bichrysophanol, which achieves an impressive binding score of -10.8 kcal/mol.
Conclusion: Despite the need for further research to identify active ingredients and elucidate their modes of action, these results suggest *E. spectabilis* as a dual-action option for cancer therapy.

Keywords: *Eremurus spectabilis,* hepatocellular carcinoma, cytotoxicity, antiangiogenic, molecular docking

3. INTRODUCTION and OBJECTIVE

Hepatocellular carcinoma (HCC) is the fourth most significant cause of cancer mortality and the seventh most frequent kind of cancer worldwide (Wang et al., 2021). In terms of primary liver cancer, HCC is the most common kind, accounting for around 80 percent of all newly diagnosed cases (R. X. Zhu et al., 2016). On a yearly basis, more than 800,000 people throughout the world are diagnosed with liver cancer, yet the incidence rates of hepatocellular carcinoma (HCC) vary greatly depending on the geographic area (Suresh et al., 2020).

Numerous etiological factors, particularly the hepatitis C virus (HCV) and the hepatitis B virus (HBV), can cause damage to the liver, resulting in the emergence of hepatocellular carcinoma (HCC) through the processes of liver fibrosis and cirrhosis, which can persist for extended periods. HCC is difficult to diagnose and treat in its early stages due to its complicated pathophysiology and the molecular heterogeneity of the disease (Sanyal et al., 2010). Options such as radiofrequency ablation, liver transplants, and surgery may result in long-term survival for individuals with early-stage HCC. Patients with advanced HCC often get systemic treatments; however, their efficacy is restricted (Jamshidi-Parsian et al., 2018).

The development and spread of HCC, a solid tumor, depends on the establishment of many blood vessels, particularly in its mature stages (Jamshidi-Parsian et al., 2018). Two primary mechanisms contribute to the rise in tumor vascularity: the recruitment of pre-existing vessels by the expanding tumor mass and sprouting angiogenesis. The main mechanism for creating new blood vessels in tumors is sprouting angiogenesis, which greatly accelerates tumor development and metastasis. For malignancies to get nutrition, oxygen, and waste products, angiogenesis—the formation of new blood arteries from preexisting endothelial cells (ECs)—is crucial. When a tumor grows beyond 1–2 mm in diameter, the available oxygen and nutrients become insufficient. This causes the balance to change in favor of pro-angiogenic factors, which in turn stimulates angiogenesis. These factors stimulate ECs to proliferate and migrate from surrounding vessels (Yao et al., 2023).

VEGF, a crucial angiogenic factor, is often overexpressed in tumors, leading to greater expression in the tumor's endothelial cells than in the hepatic parenchyma that is not tumorous (Yoshiji et al., 1999). The VEGF family includes five ligands: VEGFA, VEGFB, VEGFC, VEGFD, and VEGFE. Among these, VEGFA, VEGFB, VEGFC, and VEGFD bind to VEGFR2, which is expressed in virtually all endothelial cells and initiates their proliferation and migration, thereby boosting angiogenesis (Yao et al., 2023). In HCC, elevated levels of circulating plasma VEGF are linked to a poor prognosis, emphasizing the significance of anti-angiogenic drugs that target VEGFR directly for inhibiting tumor growth and metastasis (Yoshiji et al., 1999).

Since HCC is hypervascular, anti-angiogenic therapy is seen as a potentially effective treatment approach. The first tyrosine kinase inhibitor (TKI), sorafenib, is authorized as a common first-line therapy for advanced HCC. Additionally, lenvatinib has been authorized for use as a first-line therapy, and regorafenib is suggested as a second-line treatment for patients who have progressed after receiving sorafenib. There is also the possibility of using cabozantinib as a second-line therapy (Yao et al., 2023). Although anti-angiogenic agents are commonly used in treating HCC and have shown some positive effects, the improvement in survival rates is limited (Ribatti et al., 2019). Therefore, novel strategies are required to prevent HCC-induced angiogenesis as well as growth. These treatments are also expected to prevent the negative consequences of traditional chemotherapy, such as hair loss and bone marrow suppression (Semela & Dufour, 2004).

Natural compounds originating from plants are still being investigated by researchers in order to identify whether or not they have any therapeutic or preventative impact on the proliferation of cancer cells and angiogenesis (Bender & Atalay, 2018). Within this context, the impact of *Eremurus spectabilis* on hepatocellular carcinoma (HCC) and angiogenesis is investigated.

The genus Eremurus, part of the family Xanthorrhoeaceae, is represented in Turkey by two species: *Eremurus cappadocicus* (Turkish name Mor çiriş) and *Eremurus spectabilis* (Turkish name Çiriş) (*Bizim Bitkiler*, 2024). The plant is used as a fresh and dried vegetable and has been utilized extensively in traditional medicine. The role it plays in treating gastrointestinal disorders, liver problems, diabetes, skin conditions including scabies,

syphilis, and rheumatism, as well as various inflammatory conditions, has been noted by ethnobotanical and ethnopharmacological research (Bayrak & Yanardağ, 2021). Phytochemical investigations have found numerous metabolites in Eremurus species, including anthraquinones, coumarins, terpenoids, flavonoids, and naphthalene (Farhadi et al., 2023). In research carried out in 2013, several substances, including bianthraquinones (7,10′-bichrysophanol, chrysalodin), anthraquinones (chrysophanol, chrysophanol-8-methyl ether, aloe emodin), and a steroidal molecule (daucosterol), were identified from the chloroform extract of *E. spectabilis* (Koldas, 2023). Another study used the young leaves of *E. spectabilis* to separate methyl linolenate (1), chrysophanol (2), β-sitosterol (3), isoorientin (4), inosine (5), and sucrose (6) (Karakaya et al., 2017).

Extracts from *E. spectabilis* (hexane, ethyl acetate, and water fractions derived from methanol extract) were evaluated for antitumor efficacy versus many cell lines, including A-549 (human alveolar adenocarcinoma), MCF-7 (human breast adenocarcinoma), mPANC96 (human pancreatic adenocarcinoma), U87MG (glioblastoma), PC3 (prostate), CaCo-2 (colon), and HEK293 (human embryonic kidney cells). Nevertheless, none of the fractions exhibited anticancer properties (Karakaya et al., 2017). In a different investigation carried out by Tuzcu and other colleagues, ethanol, acetone, and water extracts from the leaves and roots of *E. spectabilis* have been shown to have cytotoxic effects against human prostate cancer (PC) (Tuzcu et al., 2017). Despite all of these results, the anticancer activity of *E. spectabilis* against the Hep3B cell line has not been documented in any of the research that has been published over the years.

This study's objective is to examine the antiproliferative and anti-angiogenic effects of various *E. spectabilis* fractions on HCC. In order to further understand the potential therapeutic benefits of *E. spectabilis*, we also conducted docking experiments to determine how various phytochemicals from the plant interact with and bind to VEGFR2.

4. BACKGROUND

4.1. Cancer

Cancer comprises a collection of disorders characterized by the unregulated growth of atypical cells capable of invading adjacent tissues & extending to other body areas (Yadav & Mohite, 2020).

A supracellular design in humans assists in controlling cell proliferation, which is necessary for growth and adaptability. Cancer is traditionally viewed as unregulated cell division that causes malignancy, invasion, and metastasis. Uncontrolled proliferation can result from somatic mutations or epigenetic alterations impacting gene expression. Additional explanations include the maturation arrest theory, cancer stem cell hypothesis, and embryonal rest theory (Motofei, 2022).

4.2. Carcinogenesis

Carcinogenesis is a multi-step, intricate process that is impacted by metabolic, genetic, and environmental factors. It involves changes in cells and molecules at the genetic and epigenetic levels. These alterations lead to the gradual emergence of cancer hallmarks, which eventually leads to the formation of fully developed metastatic cancer. Usually, the procedure is divided into three primary phases: initiation, promotion, and progression (Koya & Ibrahim, 2024).

Cancer is initiated when a cell gains a growth or survival advantage as a result of genetic mutations or epigenetic alterations. These mutations, which are either hereditary or acquired, result in irreversible DNA damage, which serves as the foundation for the development of cancer. The initiated cell may not exhibit immediate detrimental effects; however, it has the potential to develop into a neoplastic cell in the future (Koya & Ibrahim, 2024; Vogelstein & Kinzler, 2004). These initiated cells proliferate during the promotion stage, which is facilitated by factors such as chronic inflammation or hormones, resulting in the formation of tumors (Weinberg, 2007). The accumulation of additional mutations, which increases the aggressiveness of the tumor and the likelihood of metastasis, is a component of progression (Hanahan & Weinberg, 2011).

4.2.1. DNA damage in carcinogenesis

Damage to DNA is the primary cause of cancer. Mutations that induce cancer may result from DNA damage that is not rectified. DNA is influenced by both internal and extrinsic factors (Hoenerhoff et al., 2022). Internal factors include the generation of highly reactive hydroxyl radicals (•OH) formed from hydrogen peroxide and iron during oxidative stress, causing DNA damage. Furthermore, methyltransferase enzymes generate numerous methylated guanine and adenine residues, which impede DNA transcription and repair (Chatterjee & Walker, 2017). External factors like radiation, chemicals, and pollutants also contribute to DNA degradation (Berg et al., 2023). In the event that apoptosis or healing processes are unsuccessful, malignant cells may develop. Additionally, the stimulation of oncogenes or the repression of tumor-suppressing genes can be facilitated by aberrant DNA methylation or histone alterations. It thus speeds up the development of cancer (Koya & Ibrahim, 2024) (Figure 1).

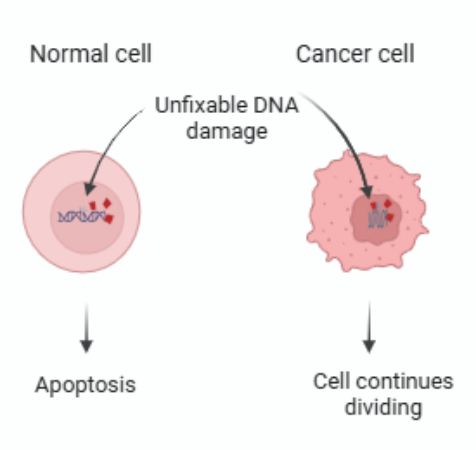


Figure 1. Illustration of DNA damage and its progression to cancer if repair mechanisms fail (BioRender, 2024).

4.3. Hepatocellular Carcinoma (HCC)

Globally, hepatocellular carcinoma (HCC) ranks as the third most common cause of cancer-related mortality. Estimates suggest that by 2025, more than a million people will receive a liver cancer diagnosis annually (Llovet et al., 2016). About 80% of primary liver cancers are HCC, with cholangiocarcinoma (10–20%) and angiosarcoma (1%) making up the remaining types (R. X. Zhu et al., 2016). Around the world, more than 800,000 individuals have been identified as having liver cancer annually, and incidence rates of hepatocellular carcinoma (HCC) vary significantly by geographic location (Llovet et al., 2016). Northern Europe and South-Central Asia have the lowest incidence rates, whereas Eastern Asia and sub-Saharan Africa have the highest rates, followed by Southern and Western European nations, North America, and Central America (Duan et al., 2019; McGlynn et al., 2015). Liver damage resulting from various etiological factors, particularly hepatitis C virus (HCV) and hepatitis B virus (HBV), promotes the development of HCC through the processes of liver fibrosis and cirrhosis, which may persist for extended periods (Figure 2). The complex pathogenesis and molecular heterogeneity of HCC impede its early diagnosis and treatment (Fernández-Palanca et al., 2019; Sanyal et al., 2010). Despite notable progress in diagnostic and therapeutic methods, the 5-year survival rate for hepatocellular carcinoma (HCC) is 18%, which is the second lowest after pancreatic cancer, and the prognosis remains poor (Jemal et al., 2017; Wang et al., 2024). High rates of tumor recurrence limited therapeutic choices for advanced HCC, and late-stage diagnosis all contribute to the poor prognosis. To enhance patient outcomes, new diagnostic and prognostic biomarkers must be found immediately, and tailored treatments must be created (Wang et al., 2024).

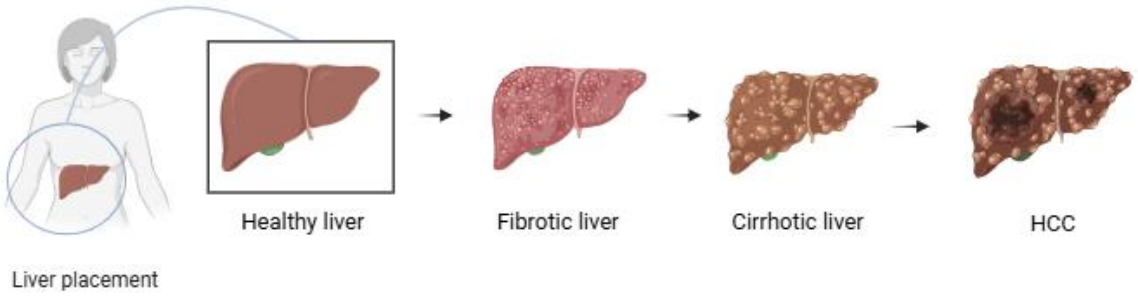


Figure 2. Progression of hepatocellular carcinoma (HCC) (BioRender, 2024).

4.3.1. HCC etiology

Hepatocellular carcinoma (HCC) is a complex biological process that involves several factors that disrupt the balance between the inactivation and activation of tumor suppressor genes and oncogenes, as well as the abnormal activation of molecular signaling pathways, HCC cell differentiation, and angiogenesis regulation (Wang & Deng, 2023). The most frequent etiological factors for the emergence of HCC are hepatitis B, hepatitis C, alcoholic liver disease, and non-alcoholic liver steatohepatitis/non-alcoholic fatty liver disease.

A. Viral hepatitis

More than 70% of cases of HCC are caused by chronic infections with the hepatitis B and hepatitis C viruses. In particular, HBV is responsible for approximately 56% of HCC cases worldwide, while HCV accounts for approximately 20% (Mohammed & Kaka, 2007).

The Hepadnaviridae family includes the circular, enclosed Hepatitis B virus (HBV), which has partially double-stranded DNA. HBV is the primary cause of chronic hepatitis on a global scale, influencing approximately 250 million individuals. The incorporation of HBV's genome into the DNA of the host is a critical mechanism by which it contributes to the development of liver carcinoma. In particular, HBV can insert its DNA into the promoter regions of telomerase reverse transcriptase (TERT) in the human genome. This can result in mutations linked to 60% of cases of hepatocellular carcinoma (Schulze et al.,

2016). Other genetic mutations seen in HBV-associated HCC include those in TP53, which influences the cell cycle; CTNNBI (beta-1 catenin); AXINI (axis inhibitor-1); ARID1A and ARID2, both involved in chromatin regulation (Mohammed & Kaka, 2007). HCC can develop in patients infected with HBV without developing cirrhosis, although cirrhosis is present in almost 80% of HBV-associated instances of HCC (Thiele et al., 2014). Co-infections with hepatitis C virus (HCV) or hepatitis delta virus (HDV) increase the chance of HCC even more (Asafo-Agyei & Samant, 2023).

The hepatitis C virus (HCV) is a single-stranded, positive-sense RNA virus that has eleven main genotypes and fifteen subtypes. Genotype 1b is often linked to HCC (Asafo-Agyei & Samant, 2023; Singh et al., 2018). Unlike HBV, HCV does not enter the DNA of the host; instead, cirrhosis plays an essential role in HCV-related liver cancer development. Chronic inflammation in HCV infection, together with fibrosis, cellular apoptosis, and regeneration, creates a milieu favorable for HCC.

Although a lower fraction of HCV-associated HCC cases occurs in people without cirrhosis (Nash et al., 2010), the majority occur in patients with severe fibrosis or cirrhosis (Lok et al., 2009). HCV causes about 20% of HCC cases worldwide, and co-infection with HBV greatly increases the chance of developing HCC (Asafo-Agyei & Samant, 2023).

B. Non-alcoholic fatty liver disease (NAFLD)

Triglycerides accumulate abundantly in liver cells in non-alcoholic fatty liver disease, resulting in steatosis even in the absence of substantial alcohol use (Engin, 2017). Patients with metabolic syndrome often have NAFLD, a condition associated with insulin resistance, high blood pressure, elevated triglycerides, and abdominal obesity, all of which heighten the risk of cardiovascular disease (Asafo-Agyei & Samant, 2023; Grundy, 2004). Today, NAFLD is recognized as a primary cause of HCC globally, particularly in Western nations (Asafo-Agyei & Samant, 2023). Though the exact mechanism of liver damage isn't fully understood, it is thought to cause liver cell injury, inflammation, and eventually fibrosis in up to one-third of patients. Ten to twenty percent of these instances develop into cirrhosis. In the United States, NAFLD affects approximately one in five individuals and has risen in incidence over the past 20 years, making it a significant contributing factor of HCC (Massarweh & El-Serag, 2017).

C. Alcohol

Three in ten instances of HCC in the United States are linked to a history of heavy alcohol consumption. Alcohol can lead to HCC both directly and indirectly, with alcoholic cirrhosis being the second most prevalent HCC risk factor in the United States and Europe (Asafo-Agyei & Samant, 2023; Testino et al., 2014; Yang et al., 2019). Indirectly, alcohol contributes to HCC by causing cirrhosis, and it also increases reactive oxidative stress and inflammation in the liver (Asafo-Agyei & Samant, 2023; Testino et al., 2014). Consuming more than 80 grams of alcohol per day raises the risk of developing HCC by five times (Asafo-Agyei & Samant, 2023).

D. Inherited metabolic disorders

Disorders such as hereditary hemochromatosis, Wilson's disease, α1-antitrypsin deficiency, and hepatic porphyria raise the risk of hepatocellular carcinoma (HCC) considerably. These conditions cause increased inflammation and hepatocellular damage, which stimulates carcinogenesis in the liver (Suresh et al., 2020).

E. Metabolic syndrome

Seven percent of all hepatocellular carcinomas are associated with metabolic syndrome, most notably diabetes mellitus. Individuals with diabetes are 2 to 3 times more predisposed to developing HCC compared to non-diabetics, irrespective of viral hepatitis status. Hyperglycemia, insulin resistance, and the initiation of insulin-like growth factor signaling pathways are factors that connect diabetes to the etiology of HCC. Moreover, obesity raises this risk via pathways related to inflammation, oxidative stress, as well as changes in gut microbiota, establishing it as a prevalent precursor to NAFLD, which serves as another underlying HCC risk factor (Suresh et al., 2020).

F. Aflatoxins

Aspergillus parasiticus and Aspergillus flavus generate the mycotoxin aflatoxin B1. Grain contamination by the fungus is primarily seen in Sub-Saharan Africa and Southeast Asia. Carcinogenesis is predominantly via the p53 tumor suppressor gene mutation.

Aflatoxin B1 is significantly related to a higher risk of HCC in patients with HBV (Asafo-Agyei & Samant, 2023; Wu & Santella, 2012).

4.3.2. HCC diagnostic approaches

Currently, all guidelines recommend ultrasonography (US) examinations for HCC early detection, whether or not they include serum alpha-fetoprotein (AFP) evaluations. Additionally, cross-sectional imaging techniques are recommended for hepatic nodules that exceed 1 cm in size. However, the currently employed approaches for diagnosing HCC still have inadequate sensitivity and specificity, particularly during the initial stages of the condition. Advanced imaging methods are being developed with increased effort to improve the characterization of HCC nodules and increase HCC detectability. Furthermore, there is also interest in significant HCC biomarkers that may have therapeutic use (Wang & Wei, 2020).

- **Imaging**

Hepatocellular carcinoma (HCC) can be identified by ultrasonography, computed tomography, or magnetic resonance imaging (MRI).

Ultrasound (US) is a diagnostic procedure for HCC that is non-invasive, with sensitivity and specificity between 51%-87% and 80%-100%, respectively. It assesses the shape, localization, dimensions, and vascular invasion of HCC. To characterize lesions detected by non-contrast ultrasonography, contrast-enhanced ultrasound is referred to as CEUS. When it comes to detecting lesions that were previously recognized as hepatocellular carcinoma (HCC) by non-contrast ultrasonography, it has a specificity of over 97% and a sensitivity of 90%. Ultrasound is advised biannually for hepatocellular carcinoma monitoring in high-risk individuals with or without serum alpha-fetoprotein.

Computed tomography (CT) functions as a diagnostic imaging technique for detecting hepatocellular carcinoma (HCC) using triphasic CT scans, with a sensitivity of 65% and a specificity of 96% per lesion. Contrast MRI demonstrates a sensitivity of 77% to 90% and a specificity of 84% to 97%. MRI imaging, influenced by fibrosis, fat, and necrosis, may vary from isointense to hyperintense, where hyperintense images represent tumors that

have undergone complete differentiation and are isointense on T2 imaging, whereas tumors that have undergone just partial differentiation appear as isointense on T1 images (Asafo-Agyei & Samant, 2023).

- **Protein biomarkers**

Serum biomarkers provide assistance for HCC diagnosis, alongside the imaging modalities. The assessments of the biomarkers are more objective. Compared to imaging-based techniques, they are considered an additional tool, including both dysregulated proteins and mRNAs. HCC can elevate liver function tests like bilirubin, ALT, AST, ALP, and albumin, which may indicate the severity of the disease. Lab testing in more severe instances may reveal issues such as low platelets, low blood sugar, low salt, anemia, high INR, or lengthy PT. On the other hand, liver function may be normal in early HCC that has not progressed to cirrhosis. Additional tests for HCC etiology include hepatitis B surface antigen, anti-HCV antibody, alpha-1 antitrypsin, copper, and iron saturation levels (Asafo-Agyei & Samant, 2023; Wang & Wei, 2020).

In recent years, alpha-fetoprotein (AFP) has become one of the most promising and extensively researched biomarker candidates since dysregulated levels of AFP are highly correlated with HCC malignancy (Wang & Wei, 2020). Additionally, elevated levels of other biomarkers, including des-gamma-carboxyprothrombin (DCP) and lectin-bound alpha-fetoprotein, may also be observed in HCC (Asafo-Agyei & Samant, 2023).

- **Serum Alpha-Fetoprotein (AFP)**

The fetal yolk sac and embryonic liver produce a serum glycoprotein known as alpha-fetoprotein (AFP) throughout pregnancy. It is often elevated in advanced HCC. Normal AFP levels are observed in early non-cirrhotic HCC. Serum AFP has a cut-off value of 10.9 ng/ml, a sensitivity of 66%, and a specificity of 80%. In terms of HCC detection, elevated levels above 200 ng/ml have a modest sensitivity but are quite specific. In patients with concomitant hepatic disease, the specificity of HCC diagnosis at a cut-off value of 500 ng/mL is more than 90% (Asafo-Agyei & Samant, 2023).

According to the Asian HCC guidelines, serum biomarker AFP measurements for HCC surveillance in conjunction with US recommendations are suggested as diagnostic tools. However, the poor sensitivity and specificity of AFP serum tests continue to hinder its use for early HCC diagnosis. Additionally, the presence of false positives further makes it difficult to differentiate HCC from other liver-related conditions, including cirrhosis (Wang & Wei, 2020).

- **Liver biopsy**

Liver biopsy is not commonly used for hepatocellular carcinoma because of the hazards of tumor seeding, bleeding, and false negatives caused by insufficient tissue collection from the proper location. Liver biopsies have a 100% specificity and a positive predictive value, with sensitivity ranging from 66% to 93% based on tumor size (Asafo-Agyei & Samant, 2023).

4.3.3. HCC stages

In 1999, the Barcelona Clinic Liver Cancer (BCLC) approach was created to assist in managing patients with cirrhosis and HCC by considering physical state, tumor load, and liver function. The system estimates the extent of the tumor based on its size, number, and the presence of portal vein invasion or extrahepatic spread. While the Eastern Cooperative Oncology Group (ECOG) scale widely assesses functional status, the Performance Scale (PS) evaluates daily activities. The BCLC system categorizes patients into very early-stage, early-stage, intermediate-stage, advanced-stage, and terminal-stage, reflecting varying degrees of liver function and metastasis. (Llovet et al., 1999; Yang et al., 2019).

- **BCLC 0:** represents extremely early-stage hepatocellular carcinoma, which is distinguished by an ECOG performance status of 0 and a single nodule up to 2 cm in diameter. Liver function is also intact.
- **BCLC A:** refers to early-stage hepatocellular carcinoma, which is distinguished by an ECOG performance status of 0 and one or up to three nodules, each no larger than 3 cm in diameter. Liver function is also intact.

- **BCLC B:** represents intermediate-stage hepatocellular carcinoma, which is multinodular and extends beyond the early stage, with preserved liver function and an ECOG performance status of 0. This group is heterogeneous and can be further subclassified.
- **BCLC C:** clearly indicates hepatocellular carcinoma in its advanced stages, with features such as vascular invasion, extrahepatic metastases, retained liver function, and an ECOG performance grade of 1-2.
- **BCLC D:** represents In individuals with end-stage liver illness or an ECOG performance rating of 3-4, this signifies terminal-stage hepatocellular carcinoma and disqualifies them from liver transplantation surgery (Tellapuri et al., 2018; Yang et al., 2019).

4.3.4. HCC treatment approaches

Since HCC treatment is highly complex, it requires a multidisciplinary approach. The treatment method applied to patients is assessed based on the stage of the disease, and the progression of the process is arranged accordingly.

A therapy map primarily derived from the BCLC classification is utilized in the treatment process. Treatment alternatives encompass ablation, transplanting, and resection for early stages. The middle stages are reserved for chemoembolization and systemic treatments. Terminally ill individuals receive the optimal supportive care possible. The AASLD and EASL have recognized BCLC as a standard staging system; nonetheless, the BCLC approach has drawbacks, including reliance on subjective elements, especially the performance status within a specific category, and the variability in patient prognosis (Tellapuri et al., 2018).

Patients classified as BCLC 0 and BCLC A are eligible for curative interventions (resection, ablation, and liver transplantation), which yield an overall survival rate of 50% to 75% over a 5-year period. Patients classified as stage BCLC B have maintained hepatic function, absence of cancer-related symptoms, and multinodular hepatocellular carcinoma without vascular involvement or extrahepatic metastases. Transarterial chemoembolization is the standard treatment for these patients, offering survival rates of up to four years in

ideal candidates. Stage BCLC C includes patients with advanced disease who may exhibit cancer-related symptoms; however, they possess reasonably maintained liver function and may have vascular invasion or extrahepatic dissemination. For these patients, many pharmacological agents are employed as first-line therapy, and systemic treatment is advised (Ayuso et al., 2018).

The principal prognostic determinants for hepatocellular carcinoma encompass tumor dimensions and quantity, serum alpha-fetoprotein levels, histological classification, and characteristics including microvascular or macrovascular invasion and metastasis. HCC therapy selection requires a complex decision-making process that takes into account tumor load, liver dysfunction severity, medical comorbidities, and patient preferences.

- **Surgical resection**

Patients with early-stage hepatocellular carcinoma who have been identified as acceptable candidates may benefit from surgical resection as a potentially curative therapeutic option. A history of cirrhosis, the extent of underlying liver damage, tumor characteristics (including size, location, and quantity), and portal hypertension are factors that influence resectability. Patients with 1-3 unilobar lesions and mild portal hypertension are usually candidates for surgical excision, if radiographic evidence shows no extrahepatic metastases, macrovascular invasion, or synthetic malfunction (Yang & Heimbach, 2020).

- **Ablation**

Ablation is recommended for individuals with BCLC stage 0 or A tumors who are ineligible for surgical intervention. Percutaneous radiofrequency ablation serves as the primary technique, generating high intratumoral temperatures under imaging guidance to induce tumor necrosis. The extent of necrosis achieved decreases considerably for tumors bigger than 3 cm in diameter and is negatively correlated with tumor size. Radiofrequency ablation may be used as an alternative to resection as the first line of treatment in some individuals who have a single tumor that is less than 2 cm in diameter and situated in a suitable region of the liver parenchyma (Yang & Heimbach, 2020).

- **Liver transplantation**

Patients with cirrhosis and a low tumor load can benefit from liver transplantation. The criteria include either a single tumor measuring less than 5 cm or two to three tumors measuring less than 3 cm, all without any vascular invasion. It yields recurrence rates of 10–15% at 5 years and survival rates of around 70% and 50% at 10 years, respectively. Since liver transplantation treats both cirrhosis and hepatocellular carcinoma and has a far lower cancer recurrence rate than other treatment options, it is the recommended course of treatment for early-stage, unresectable hepatocellular carcinoma in cirrhotic patients (Llovet et al., 2016; Sugawara & Hibi, 2022).

- **Transarterial chemoembolization (TACE)**

This is the most popular therapy used for HCC. TACE restricts the tumor's blood supply by causing intratumoral ischemia through arterial embolization and administering cytotoxic therapy directly to the tumor (Yang & Heimbach, 2020).

- **TACE and TARE**

TACE is the primary treatment for patients with BCLC-stage B HCC. Either lipiodol (conventional TACE) or drug-eluting beads (DEB-TACE) are used to deliver therapy directly to tumors through arterial blood flow. With a median survival of 19.4 months, meta-analyses have shown that TACE considerably increases overall survival (OS). Although the mortality rate is very modest at 0.6%, common adverse effects include liver enzyme abnormalities, fever, bone marrow toxicity, discomfort, and vomiting. A different intra-arterial treatment called TARE (transarterial radioembolization with Y-90) has shown better overall survival (OS) and time to progression (TTP) in randomized controlled trials (RCTs) like TRACE. TARE optimizes treatment delivery through personalized dosimetry, increasing response and survival rates (Singal et al., 2023).

- **Systemic therapy**

Patients who exhibit progression despite transarterial therapies and have advanced disease (BCLC stage C) or intermediate-stage disease (BCLC stage B) are advised to receive systemic treatments. These treatments primarily involve antiangiogenic targeted therapies

(e.g., sorafenib, lenvatinib) and immune checkpoint inhibitors (ICIs) such as PD-1 and CTLA-4 inhibitors. While these therapies are generally well-tolerated, they can cause a range of side effects, including immune-related adverse events (Singal et al., 2023).

- **Sorafenib**

Sorafenib, the first systemic medication approved by the FDA for the management of hepatocellular carcinoma, remains the standard of care for first-line treatment. Since its approval, studies on novel targeted therapies have suggested that sorafenib is not always superior to alternative options (Ján et al., 2020).

4.4. Angiogenesis

The term angiogenesis was initially defined by English surgeon Dr. John Hunter in the late 17th century as "the formation of new blood vessels from existing blood vessels" (Figure 3). Subsequently, in 1935, pathologist Dr. Arthur T. Hertig revealed angiogenesis in the placenta of a pregnant monkey (Ribatti, 2008).

Angiogenesis manifests in the organism in two forms: physiological and pathological. Physiological angiogenesis occurs in a healthy organism during embryogenesis, placentation, wound healing, and inside the female reproductive system, such as during corpus luteum development.

Pathological angiogenesis may manifest in atherosclerosis, rheumatoid arthritis, psoriasis, chronic inflammation, inflammatory bowel diseases, tumorigenesis, and metastasis, particularly in various cancers including breast, bladder, colon, lung, neuroblastoma, melanoma, kidney, pancreas, uterus, cervix, and glioblastoma. It is also observed in juvenile hemangioma, age-related macular degeneration, diabetic retinopathy, and ocular and cardiovascular diseases (Polverini, 1995).

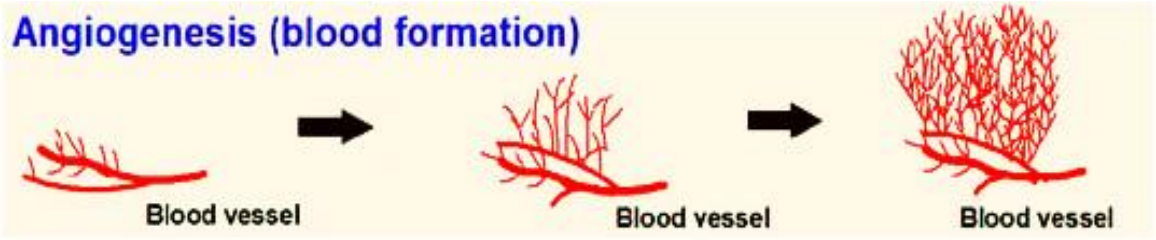


Figure 3. Angiogenesis (Rajabi & Mousa, 2017).

4.4.1. Key stages of angiogenesis

Angiogenesis is a process with many steps, including the production of proteases, the migration and proliferation of endothelial cells, the formation of vascular tubes, the joining of pericytes and smooth muscle cells, and the anastomosis of newly formed tubes. Endothelial cells produce proteolytic enzymes in response to angiogenic signals, which degrade the basement membrane and perivascular extracellular matrix (ECM). Initiation of sprouting occurs when endothelial cells multiply and move into the perivascular area as a result of this process. In due time, capillary loops will arise from these sprouts' newly formed lumens. Subsequently, a new basement membrane forms, and the blood vessels develop into structures resembling tubes, enabling blood to circulate (Rajabi & Mousa, 2017).

Organ perfusion, wound healing, and embryonic development all depend on this process. Yet, serious diseases can develop as a result of abnormal angiogenesis. Angiogenesis can also be regulated by inhibitors that act on various proteins, such as VEGF, bFGF, and TGF-β, keeping the process in check to keep the blood vessels at a steady state. In tumors, VEGF promotes angiogenesis, allowing tumor cells to nourish themselves by forming new blood vessels, although some tumors may develop alongside pre-existing vessels without causing the development of new ones (Rajabi & Mousa, 2017).

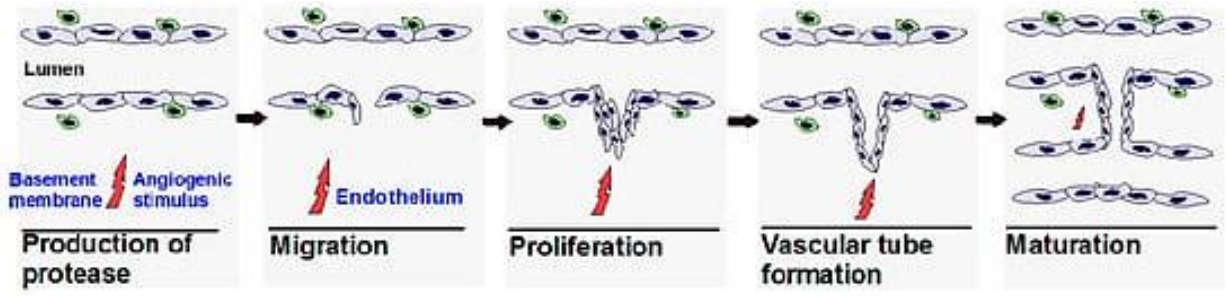


Figure 4. Steps in angiogenesis (Rajabi & Mousa, 2017).

4.4.2. Angiogenesis in pathological processes

Angiogenesis in the body is controlled by regulatory factors that are both pro-angiogenic and angiostatic (anti-angiogenic, inhibiting angiogenesis) in nature, in addition to the angiogenic stimulus (Distler et al., 2003). The ECM and surrounding cells release regulators such as growth factors (VEGF, placental growth factor [PGF]), cytokines (interleukin-1 [IL-1], prostaglandin E2 [PGE2]), their receptors, regulatory proteins, and cell adhesion molecules (Konukoğlu & Turhan, 2005). Angiogenesis normally is controlled by the balance between these regulatory factors (Iruela-Arispe & Dvorak, 1997). Disruptions in the balance of angiogenesis control mechanisms, such as metabolic stress, mechanical stress, immune/inflammatory responses, and genetic mutations, often arise in pathological conditions, especially those driven by hypoxia (Ataergin et al., 1999; Carmeliet & Jain, 2000). Angiogenesis is triggered by elevated levels or activation of angiogenic factors, along with a reduction or inactivation of angiogenesis inhibitors, with VEGF playing an important part in the development of angiogenesis-related pathologies (Paper, 1998; Yao et al., 2023).

4.4.3. Tumor angiogenesis and metastasis

In cancer, the formation of blood vessels is controlled by the oxygen level. Certain angiogenic factors such as VEGF, bFGF, EGF, and IL-8 activate the endothelial cells when the oxygen level decreases (hypoxia). These factors allow EC to grow and move, helping them form new blood vessels that supply cancer cells with oxygen and nutrients. Oxygen-sensing proteins and the HIF transcription factors play a big role in important processes like cell survival, metabolism, and angiogenesis (Rajabi & Mousa, 2017). Tumors that

exceed 0.5 mm^3 can meet their oxygen and nutrient requirements by diffusion, but once they exceed this size, they become dependent on angiogenesis (Konukoğlu & Turhan, 2005). As tumors proliferate, pro-angiogenic factors surpass the effects of inhibitors, resulting in vigorous blood vessel development. PGE2 and thyroid hormone-like factors contribute to angiogenesis, while proteins such as CCN3 promote it and CCN5 prevent it, thereby affecting tumor vascularization (Rajabi & Mousa, 2017).

4.4.4. Angiogenesis in hepatocellular carcinoma (HCC)

Hepatocellular carcinoma (HCC) is a hypervascular tumor distinguished by abnormal blood vessel formation, which facilitates its proliferation, invasion, and metastasis. The process of angiogenesis in HCC is essential for the survival and spread of tumors. This process is controlled by an equilibrium of pro-angiogenic and anti-angiogenic elements. In HCC, molecules such as VEGFA, Ang2, FGF2, and TGF-β promote angiogenesis by stimulating receptors on ECs. Hypoxia additionally enhances the production of VEGFA, whereas signaling pathways such as PI3K/AKT and MAPK are activated by interactions among leptin, FGFR1, and other angiogenic factors (Yao et al., 2023).

4.4.5. Mechanisms and inhibition of angiogenesis in HCC

Pro-angiogenic molecules like VEGFA, Ang2, FGF2, PDGFA, CXCL12, and TGF-β are released by HCC cells and interact with receptors on endothelial cells, stimulating angiogenesis. The expression of most of these molecules is additionally enhanced in hepatocellular carcinoma cells when exposed to hypoxia. Leptin enhances VEGFA expression by interacting with Ob-R in HCC cells. VEGFA interacts with VEGFR2, thus activating the PI3K/AKT and RAF/MAPK signaling pathways, therefore facilitating angiogenesis. FGF2 facilitates angiogenesis in HCC through its interaction with FGFR1, hence activating the RAF/MAPK pathway. PDGFA stimulates MEK/ERK signaling through PDGFR, hence facilitating angiogenesis. TGF-β interacts with CD105 and stimulates the ALK/SMAD1/5 signaling pathway, hence facilitating angiogenesis. COX2 and VEGFA-induced Ang2 promote angiogenesis through their interaction with the Tie2 receptor. SOX4-induced CXCL12 promotes angiogenesis through its interaction with the CXCR4 receptor. Nvp-bep800 suppresses HSP90β in endothelial cells and therefore diminishes angiogenesis in hepatocellular carcinoma. AMD3100 inhibits CXCR4 in

endothelial cells, hence reducing angiogenesis in hepatocellular carcinoma. TRC105 inhibits CD105 in endothelial cells, hence reducing angiogenesis in hepatocellular carcinoma (Yao et al., 2023).

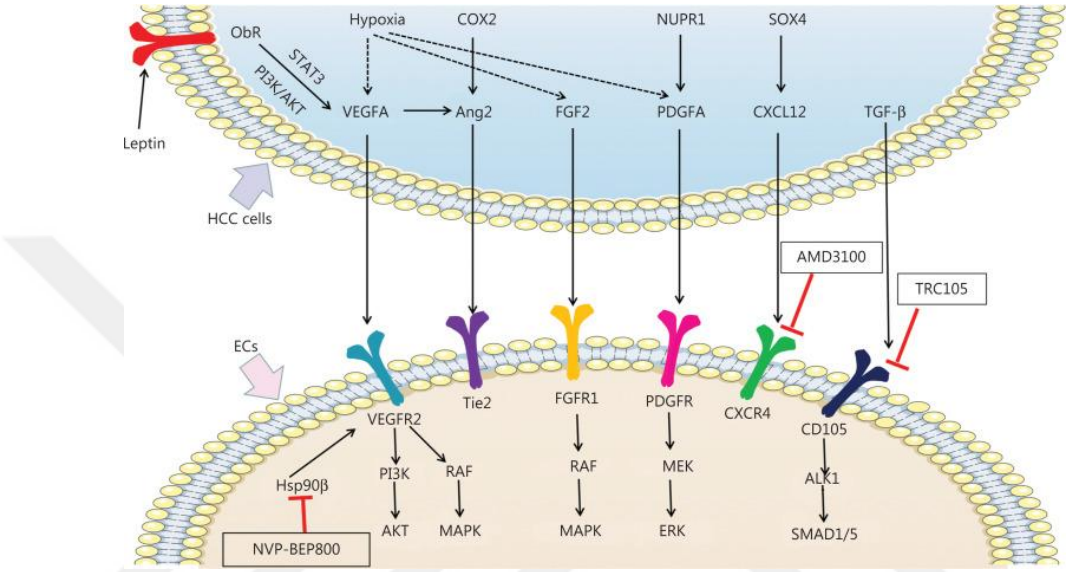


Figure 5. Mechanisms of pro-angiogenic factors inducing angiogenesis and new potential targets inhibiting angiogenesis in HCC (Yao et al., 2023).

4.4.6. Role of VEGF in angiogenesis

Endothelial cells are significantly regulated by VEGF, which is essential for tumor angiogenesis. It enhances tumor development and metastasis by facilitating the migration and proliferation of ECs. VEGF levels are elevated in HCC patients, correlating with high microvessel density and poor prognosis. The VEGF family includes five ligands: VEGFA, VEGFB, VEGFC, VEGFD, and VEGFE. Among these, VEGFA, VEGFB, VEGFC, and VEGFD bind to VEGFR2, which is expressed in almost all endothelial cells. VEGFA binds to VEGFR2, initiating a phosphorylation cascade that activates PI3K/AKT and RAF/MAPK pathways. As a result, new blood vessels are created, many of which leak, raising interstitial pressure and exacerbating tumor hypoxia, which accelerates angiogenesis and the spread of HCC (Yao et al., 2023).

4.4.7. Anti-angiogenesis therapies in HCC

Anti-angiogenic therapies targeting tyrosine kinases, VEGF receptors, and PDGFR have been introduced for treating advanced HCC. Sorafenib, Lenvatinib, and Regorafenib are approved for advanced stages, with modest survival benefits. However, these therapies have limited effectiveness, prompting the search for new targets to enhance anti-angiogenic treatment (Yao et al., 2023).

4.5. Drug Resistance in Hepatocellular Carcinoma

The tumor's substantial resistance to conventional chemotherapy is the primary reason for the poor prognosis of patients with non-operable advanced hepatocellular carcinoma (HCC). Innovative pharmaceutical strategies utilizing tyrosine kinase inhibitors (TKIs), primarily sorafenib and regorafenib, have yielded only a modest extension of overall life in patients with HCC (Marin et al., 2020).

Drug resistance mechanisms may be intrinsic or acquired. Naturally, cancer cells are unresponsive to therapies due to their intrinsic resistance. Acquired resistance occurs when cancer cells that were initially susceptible to treatment develop resistance. Drug resistance is a complex phenomenon that encompasses concurrent pleiotropic cellular signals. These include the upregulation of drug efflux, downregulation of drug uptake, sequestration of medicines, alterations in drug metabolism, aberrant production of non-coding RNAs, inhibition of apoptotic signals, modifications in the tumor microenvironment, acquisition of stem cell-like characteristics, and autophagy. A single cancer type may develop a variety of drug resistance mechanisms, which presents significant challenges to a comprehensive understanding of the signaling network (Duan et al., 2019).

With the recent clinical use of plant secondary metabolites and their derivatives in the fight against cancer, the discovery of medicines derived from medicinal plants has become vital in oncological therapy. Primary metabolites are essential macromolecules generated by plants for survival, whereas secondary metabolites are nonessential chemicals derived from primary metabolites found in plants. Secondary metabolites can be categorized into three principal groups: phenolic chemicals, terpenoids, and nitrogen-sulfur-containing compounds (Seca & Pinto, 2018).

The National Cooperative Drug Development Group (NCDDG) has played a pivotal role in drug development by employing techniques such as plant isolation, synthetic chemistry, and molecular modeling to uncover novel compounds with potential therapeutic applications. From 1981 to 2002, over 25% of the top-selling pharmaceuticals globally originated from natural products, whereas 40% of contemporary anticancer medications are derived from natural sources. Early in the 1990s, the antineoplastic medication paclitaxel was clinically introduced in the United States after being first isolated from Taxus brevifolia Nutt (Balunas & Kinghorn, 2005).

European yew tree needles contain docetaxel, a semisynthetic derivative of paclitaxel that is a potent anticancer agent. Docetaxel is approved to stabilize microtubules, induce cell cycle arrest and apoptosis, and treat anthracycline-resistant metastatic breast cancer (Montero et al., 2005). Docetaxel is widely used in treating various cancers, including advanced breast and non-small cell lung cancer. Numerous disease types have demonstrated their broad antitumor activity (Baker et al., 2006; Kenmotsu & Tanigawara, 2015). The CYP3A drug-metabolizing pathway breaks down docetaxel very quickly in the liver. This makes it a possible drug for treating liver cancer. Studies have recognized its low toxicity and high therapeutic efficacy, demonstrating its ability to reduce hepatocellular tumor size in mice and inhibit cell proliferation in the HepG2 cell line (Syn et al., 2016; Zhang et al., 2019; D. Zhu et al., 2016).

Numerous studies have described a variety of natural and phytochemical agents that have the potential to prevent or mitigate primary liver cancer and hepatic injury (Hamzawy et al., 2015). The investigation of phytochemicals derived from plants has emerged as a prospective field of research in the field of cancer. In this context, the anti-angiogenesis potency and cytotoxic activity of *E. spectabilis* on hepatocellular carcinoma (HCC) are examined.

4.6. Eremurus spectabilis

The genus Eremurus, a significant member of Xanthorrhoeaceae consisting of 62 species, is commonly referred to as foxtail lily or desert candles (Bayrak & Yanardağ, 2021). This genus is widely distributed in central and western Asia, encompassing Iran, Afghanistan, Iraq, Tajikistan, Syria, Pakistan, Lebanon, Turkey, China, and India. The Eremurus species is a perennial herbaceous plant distinguished by narrow, elongated leaves that are intricate at the base, averaging 30–70 cm in length and 1–3 cm in breadth. The roots are significant, fleshy, sturdy, and tuberous, while the blooms display a color range from white to pink, arranged in a clustered spike (Farhadi et al., 2023).

Two Eremurus species, *Eremurus cappadocicus* (Turkish name Mor çiriş) and *Eremurus spectabilis M. Bieb* (Turkish name Çiriş), grow naturally and are found in the Mediterranean, East, and Southeast areas of Turkey (the Eastern Anatolian part of Turkey). Historically, people have used *E. spectabilis*, both fresh and dried, as a wild edible vegetable and as a traditional medicinal remedy. Ethnobotanical and ethnopharmacological investigations have demonstrated its application in the traditional treatment of gastrointestinal pain, liver disorders, diabetes, scabies, syphilis, rheumatism, and various inflammations. According to phytochemical investigations, flavonoids, terpenoids, anthraquinones, coumarins, and naphthalene have been found in Eremurus species (Bayrak & Yanardağ, 2021). Recently, a study conducted in 2023 reported the isolation of several compounds from the chloroform extract of *E. spectabilis*, these compounds including bianthraquinones (7,10′-bichrysophanol and chrysalodin), anthraquinones (chrysophanol, chrysophanol-8-methyl ether, aloe emodin), and the steroidal compound daucosterol (Koldas, 2023). Another study also documented the isolation of methyl linolenate (1), chrysophanol (2), β-sitosterol (3), isoorientin (4), inosine (5), and sucrose (6) compounds from the young leaves of *E. spectabilis* (Karakaya et al., 2017).



Figure 6. *Eremurus spectabilis*.

4.6.1. Previous studies on anticancer effects of *E. spectabilis*

Extracts from *E. spectabilis* (hexane, ethyl acetate, and water fractions derived from methanol extract) were tested for anticancer activity against several cell lines, including A-549 (human alveolar adenocarcinoma), MCF-7 (human breast adenocarcinoma),

mPANC96 (human pancreatic adenocarcinoma), U87MG (glioblastoma), PC3 (prostate), CaCo-2 (colon), and HEK293 (human embryonic kidney cells). Nevertheless, none of the fractions exhibited anticancer properties (Karakaya et al., 2017). In another study conducted by Tuzcu and other colleagues, ethanol, acetone, and water extracts from the leaves and roots of *E. spectabilis* have been shown to exhibit cytotoxic effects against human prostate cancer (PC) cell lines (Tuzcu et al., 2017).

A further investigation carried out by Abubaker and Hidayat revealed that both water and hexane-ethanol extracts of *E. spectabilis* displayed antiproliferative effects against different cancer cell lines due to their bioactive components (e.g., carvacrol, cadelene, valence). These effects may be ascribed to the plant's abundance of phenolics and flavonoids (Bayrak & Yanardağ, 2021).

Despite all of these results, the anticancer activity of *E. spectabilis* against HCC has not been documented in any of the research that has been published over the years.

4.6.2. Nutritional, antioxidant, and antimicrobial properties of *E. spectabilis*

E. spectabilis (young leafy plant) shows a significant nutritional value for its chemical composition. The protein, potassium, calcium, magnesium, iron, and copper levels of *E. spectabilis* were shown to be superior to those of several other regularly utilized vegetables, suggesting that it may fulfill the daily requirements for these nutrients in an adult. *E. spectabilis* also exhibited considerable antioxidant and free radical scavenging properties. The free radical scavenging capability may be one route by which this plant serves as a natural antioxidant (Tosun et al., 2012).

The investigation into the antioxidant and antibacterial properties of *E. spectabilis* young leaves indicates favorable effects on DPPH radical-scavenging capacity. The aqueous extract of *E. Spectabilis* exhibits antifungal and antibacterial properties against Candida albicans and Staphylococcus aureus infections, whereas the ethyl acetate extract (residue) possesses the highest total phenolic content and the most effective antioxidant activity. The findings of this study suggest that the aqueous extract of *E. spectabilis* may provide protection against infections caused by Candida albicans and Staphylococcus aureus (Taskin et al., 2012).

4.6.3. Therapeutic activities of *E. spectabilis*

The leaves and roots of *E. spectabilis M.Bieb* exhibit gastroprotective, antidiabetic, dermal infection-healing, and antihyperlipidemic activity (Jahanbin et al., 2017).

4.6.4. Bioactive compounds isolated from *E. spectabilis*

The isolated phytochemicals from *E. spectabilis* documented in the literature are listed below (Karakaya et al., 2017; Koldas, 2023; *Pubchem*, 2024)

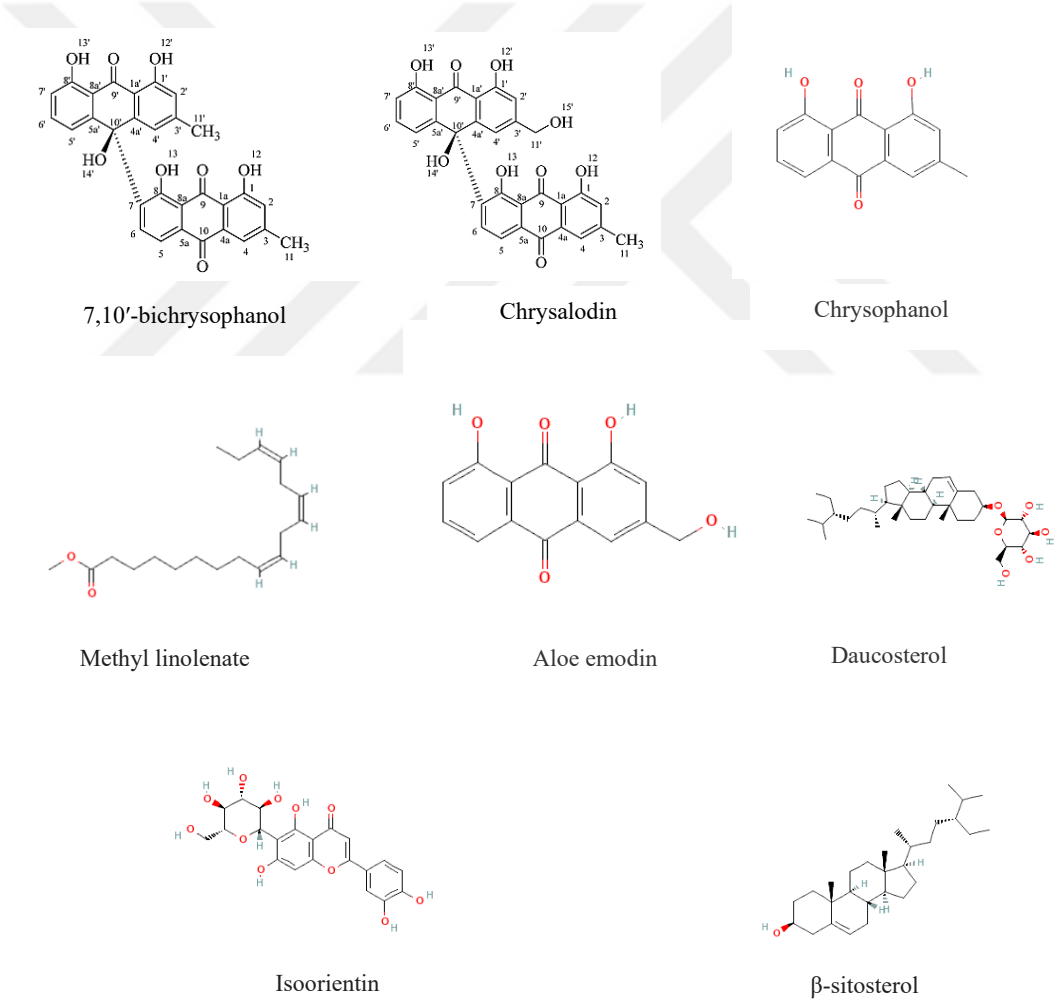


Figure 7. Chemical structures of compounds isolated from *E. spectabilis.*

5. MATERIALS and METHODS

5.1. Materials

Devices

- Camera System
- CO_2 Incubator (MCO-19AIC (UV))
- Dremel Hand Drill (Dermel)
- Freezer (-20°C) (Uğur)
- Freezer (-80°C) (Panasonic, Japan)
- Incubator (37°C) (Heraus)
- Inverted Microscope (Olympus CKX)
- Ikosa (Ikosa)
- Micropipettes (Gillson-Thermo-Eppendorf)
- Refrigerated Centrifuge (Universal 32R Hettich)
- Rotary Evaporator
- Separation Funnel
- Ultrapure Water System (Ultra Pure Type I Water)
- Vortex (IKA MS2)
- Whatman Paper, 1mm Thickness (Whatman)
- Xcelligence RTCA (Roche)

Chemicals

- Bovine Serum Albumin (BSA) (Sigma)
- Dimethyl Sulfoxide (DMSO) (Santa Cruz)
- Ethanol (Sigma Aldrich, USA)
- Fetal Bovine Serum (FBS) (Gibco)
- Fertilized Egg (Paktavuk)
- Hank's Balanced Salt Solution (PBS) (Gibco)

- Penicillin/Streptomycin (Sigma Aldrich, USA)
- Phosphate Buffered Saline (PBS) (Gibco)
- Trypsin-EDTA (Thermo Fischer)

Plant material: The above-ground parts of *E. spectabilis* were acquired from the local market in the Üsküdar area of Istanbul in March 2019, and the plant was identified by Dr. İsmail Şenkardeş (MARE No. 22262).

5.2. Extraction Process

The aerial parts of *E. spectabilis* were freshly chopped into small pieces, and the extraction process was started with 96% ethanol. The extraction process was continued until the solvent was decolored. A portion of the ethanol extract, which was filtered and evaporated in the rotary evaporator, was taken and dissolved with the minimal quantity of 50% ethanol it could dissolve in and transferred to the separation funnel. It was then extracted with hexane, chloroform, and ethyl acetate solvents, respectively. The rotary evaporator evaporated the solvents of the obtained fractions at a temperature not exceeding 45 °C, yielding hexane (ESH), chloroform (ESC), ethyl acetate (ESEA), and aqueous ethanol (ESAE) fractions. We stored the obtained fractions at +4 °C until analysis.

5.3. Hep3B Cell Culture and Handling Procedures

In this study, Hep3B cell lines, a human-derived model for hepatocellular carcinoma with the hepatitis B virus integrated into its genome, were used. These cells were cultured in DMEM supplemented with FBS, L-glutamine, penicillin-streptomycin, and non-essential amino acids and incubated at 37°C in a humidified atmosphere with 5% CO_2.

5.3.1 Cell thawing

Cell lines stored in 2 ml aliquots at -80°C were thawed in a 37°C water bath until fully liquefied. The thawed cells were placed into a 15 ml Falcon tube, combined with 5 ml DMEM, and centrifuged at 1800 rpm for 5 minutes. After discarding the supernatant, the cells were resuspended and transferred to 75 cm^2 culture flasks. The date and cell information were labeled on the flasks, which were then placed in the incubator.

5.3.2. Cell passaging

Cells in the flasks were passaged when they reached 80% confluence. The passage process was repeated every 2-4 days, depending on cell growth rate. To start the passaging process, the medium was poured into the waste container, and the flasks were washed with 5-6 ml PBS. Then, a sufficient amount of trypsin-EDTA solution was applied dropwise to cover the surface. Cells treated with trypsin were placed in an incubator. After an average of 2-3 minutes, the cells were removed and examined under a microscope. When cells were seen detaching from the surface, 2-3 ml of medium was added to inhibit trypsin. After adding an additional 5 ml of medium, the supernatant was removed by centrifugation at 1800 rpm for 5 minutes. The cell pellet was suspended in 1 mL of medium. Next, 200-500 µl of the suspension was transferred to a flask with 12-14 ml of fresh medium.

5.3.3. Cell counting

After detaching the cells from the surface with trypsin-EDTA, they were transferred to Falcon tubes containing approximately 5 ml of medium. After 10 minutes of centrifugation at 1800 rpm, the supernatant was discarded, and 1 ml of medium was added to create a suspension. A 1:100 dilution was achieved by mixing 10 µl of the suspension with 990 µl of PBS in a 2 ml Eppendorf tube. A sufficient amount of this suspension was used to cover the Thoma slide and counted using a microscope at 10X magnification. Cells were counted in the area denoted by the letter "E" (Figure 8). This area is found in two compartments on the Thoma slide, and each was counted separately to calculate an average. The cell count per 1 ml was calculated using the formula shown below.
Cell count per 1 ml = average cell counts x 10000 x 100 (dilution factor).

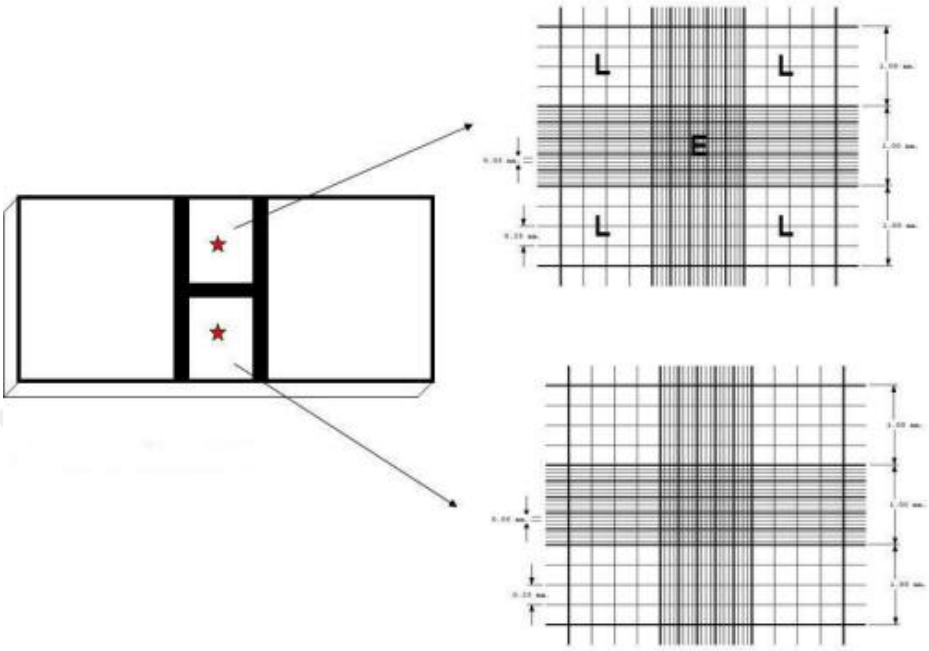


Figure 8. Thoma slide used for cell counting external and microscopic views.

5.3.4. Cell freeze

After detaching the cells from the surface with trypsin-EDTA, they were centrifuged for 10 minutes at 1800 rpm with 5 ml of fetal bovine serum. After removing the supernatant, cells were suspended in 9500 µl of fresh fetal bovine serum with 500 µl of DMSO (5% dimethyl sulfoxide). The cells were quickly aliquoted into 2 ml vials and frozen at -20°C for about 30 minutes before being transferred to a -80°C freezer for storage.

5.4. Cell Viability Assay with Xcelligence® RTCA Assay

The Xcelligence System Real-Time Cell Analysis method is used to determine cytotoxicity. It employs microelectrodes to measure changes in electrical impedance caused by cells adhering to the base of the plates in which they are grown. These changes are transmitted to a detector via electrodes, which records them synchronously through an interface, providing quantitative data on cell proliferation. The device has disposable wells (E-plate/well plate) that are used only once to seed cells and test desired substances.

Preparation of Cells: Flasks with a surface area of 25 cm^2, where the cells were cultured, were observed under an inverted microscope (Olympus CKX41). When the cells reached approximately 80% confluency, they were prepared for the experiment. After washing with PBS, trypsin-EDTA was added in sufficient quantity to cover the surface, allowing the cells to detach from the flask. The detached cells were collected in 15 mL tubes and centrifuged at 1800 rpm for 10 minutes along with the culture medium. The resulting pellet of cells at the bottom was resuspended by adding 1 mL of culture medium.

The cell count in 1 mL of volume was determined using a Thoma chamber after diluting the cells with PBS. The number of cells to be seeded was determined as an average of 1×10^4 cells per well for Hep3B, and the time period for logarithmic cell growth was selected.

Preparation of the Device: One day before the experiment, the Real-Time Cell Analyzer device was cleaned with 70% technical alcohol and put in the incubator to achieve temperature balance. To begin the experiment, 100 µl/ml of cell culture medium was added to the E-plate (16 wells per plate) for the device. Following its placement in the device, a background measurement was taken. In this measurement, the electrical difference caused by the culture medium was recorded as zero in the device. Following the measurement, the device's message section was checked. If there was a problem in the wells, error messages were recorded, and the device contact points were cleaned with a device-provided brush, or the cell seeding process was repeated.

After the device was ready, the prepared Hep3B cells were added to the E-plates removed from the device at the desired number (100 µL per well). At this point, the E-plates were kept in the safety cabinet for about 30 minutes. After incubating the cells for 24 hours and confirming their natural growth, we supplemented the wells with hexane (ESH), chloroform (ESC), ethyl acetate (ESEA), and aqueous ethanol (ESAE) fractions at concentrations of 100, 50, and 10 µg/mL. The wells were subsequently incubated for an additional 72 hours, and impedance readings were obtained every 15 minutes during the 96-hour incubation period. The IC_{50} values of each fraction were determined using the xCELLigence® RTCA data and the GraphPad Prism 5 software (Figure 8).

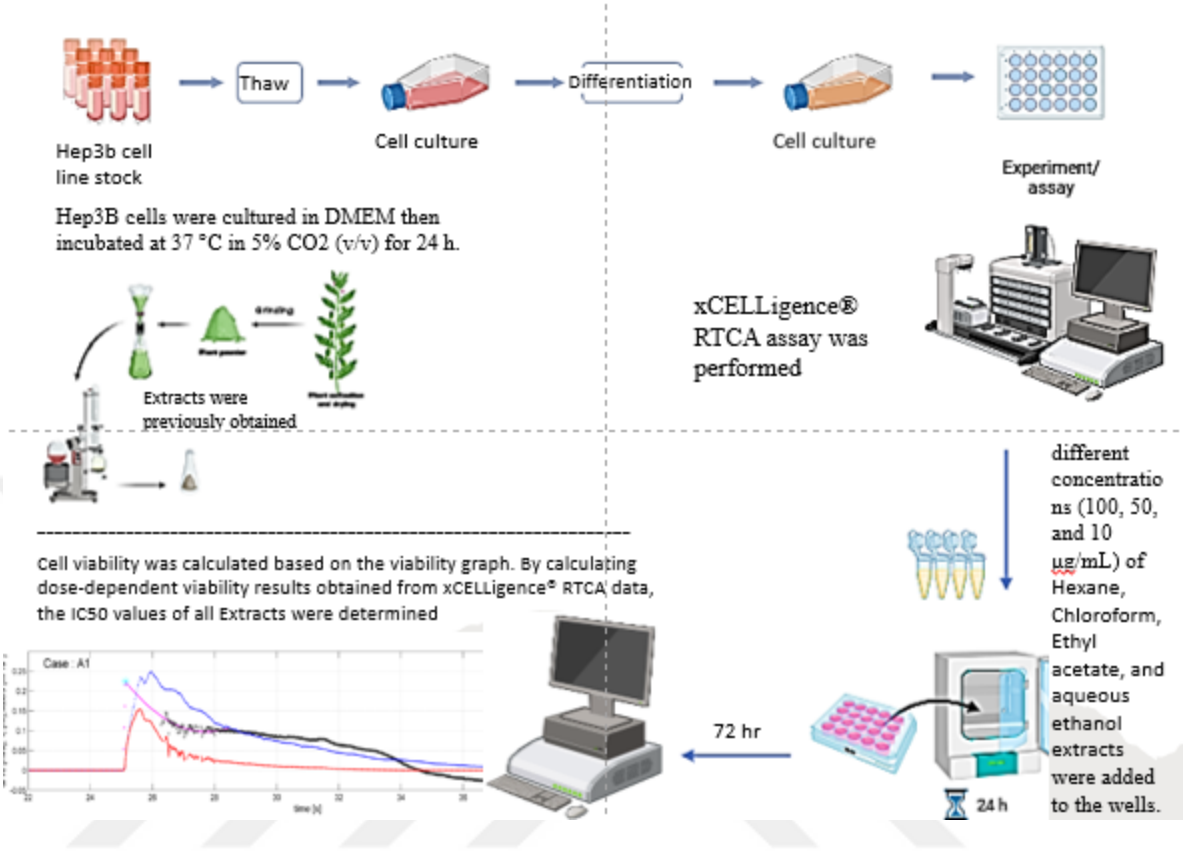


Figure 9. illustration of the methodology (BioRender, 2024).

5.5. The Chick Embryo Chorioallantoic Membrane (CAM) Assay

The chorioallantoic membrane (CAM) is formed by the fusion of the mesodermal layers of the allantois and chorion during avian development. The CAM swiftly expands and establishes a dense vascular network. This structure facilitates the investigation of tissue grafts, tumor growth, metastasis, drug delivery, toxicologic analysis, and angiogenic and anti-angiogenic molecules. The CAM is a low-cost, fast, and straightforward model that enables the rapid screening of many pharmacological samples and does not necessitate the completion of administrative procedures to obtain ethics committee approval for animal experimentation.

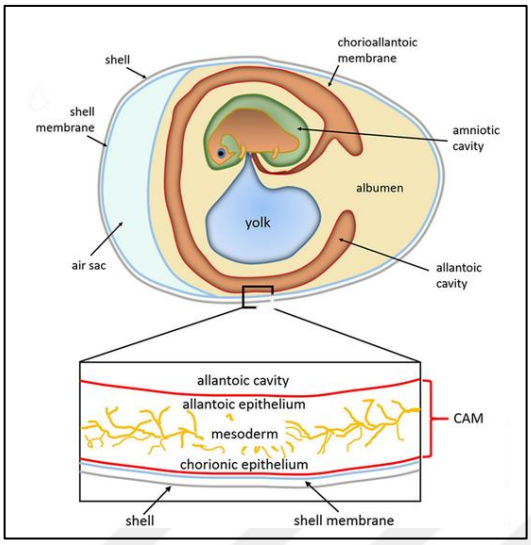


Figure 10. A schematic illustration of the chick chorioallantoic membrane (CAM) and the general structure of a five-day-old chick embryo in the egg (Rezzola et al., 2020).

At approximately 3-5 days of incubation, the chick embryo's allantois emerges as an evagination from the ventral wall of the endodermal hind intestine. The mesodermal layer of the allantois fuses with the adjacent mesodermal layer of the chorion to form the chorioallantoic membrane (CAM), and the allantoic vesicle enlarges swiftly from days 4-10 of incubation. This double layer establishes an exceptionally extensive vascular network that is linked to the embryonic circulation by two allantoic arteries and one allantoic vein.

The angiogenic process in the zone between the chorionic epithelium and the mesodermal blood vessels is enhanced by the remodeling of the CAM's extracellular matrix through the expression of fibronectin, laminin, and type IV collagen. Prior to day 6 of incubation, the CAM serves as a repository for waste materials ejected by the embryo as well as conducting gas exchange processes (Ribatti, 2017). In this research, the CAM model was used to investigate the anti-angiogenic effect of *E. spectabilis* different fractions.

Fertilized ROSS308 chicken eggs are incubated at 37°C with 60% humidity until embryonic development day three (EDD3). On EDD3, 3 mL of albumin was withdrawn from the eggs and returned to the incubator (Figure 11). On EDD4, the tops of the eggs were opened in a circular shape with a diameter of 1-2 cm, wrapped with adhesive tape,

and returned to the incubator (Figure 12). The viability of the embryos was monitored in the following days.

The fractions at the appropriate concentrations (with a minimum of six eggs per group) were applied to the CAM layer on EDD6 by impregnating sterile filter paper discs with a diameter of 6 mm and placing them on the grouped eggs (Figure 13). The CAM layer was photographed immediately following application (0 hours) and 24 hours later. The KML Vision IKOSA® CAM Assay 3.0.0 was employed to analyze the images that were obtained. The data obtained from the analysis were represented as a factor increase in comparison to the zero-hour measurement.

Each *E. spectabilis* fraction was tested for 24 hours at doses matching the IC_{50} value derived from the cell viability assay on the cell line and half of this value ($IC_{50/2}$).



Figure 11. Monitoring embryo viability.



Figure 12. Removal of 3 mL of albumin from eggs on embryonic day 3 (EDD3).



Figure 13. Circular opening (1-2 cm in diameter) created on the tops of eggs on embryonic day 4 (EDD4).

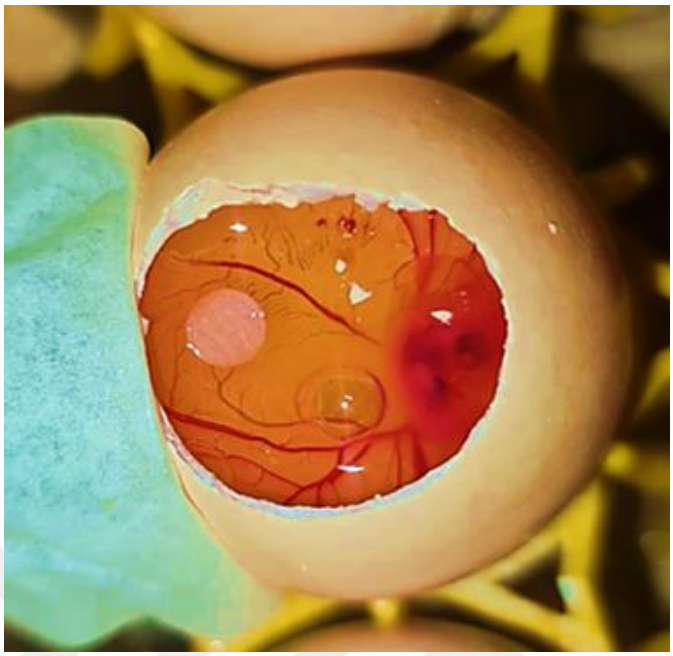


Figure 14. Fractions were applied to the CAM layer on EDD6 using 6 mm sterile filter paper discs.

5.4. Docking

Many software and web-based servers have been developed for analyzing molecular docking processes. Among these, AutoDock Vina is frequently used due to its free availability. In our study, Chimera 1.14 and AutoDock Vina were utilized as the docking preparation tool and engine, respectively. Additionally, a server developed by Salentin et al. in 2015 (https://projects.biotec.tu-dresden.de/plip-web/plip/index) was used to analyze hydrogen bond interactions.

For the molecular modeling study, the enzyme VEGFR2 (PDB ID: 2OH4) was downloaded in PDB format from the Protein Data Bank (https://www.rcsb.org/structure/2OH4). The structural crystallographic form of VEGFR2 originates from *Homo sapiens* and consists of a single main chain. The selected compounds were those previously identified from *E. spectabilis*, which were downloaded from the PubChem database and prepared for docking analysis (PubChem). The objective was to investigate the binding of these compounds to VEGFR2, the types of interactions, and their binding energies using computational docking techniques to gain a deeper understanding of the plant's anti-angiogenic mechanisms.

A. Protein Preparation

The crystallographic structure of VEGFR2 (PDB ID: 2OH4) was obtained from the Protein Data Bank (https://www.rcsb.org/structure/2OH4). This structure, derived from *Homo sapiens*, consists of one main chain (Figure 14).

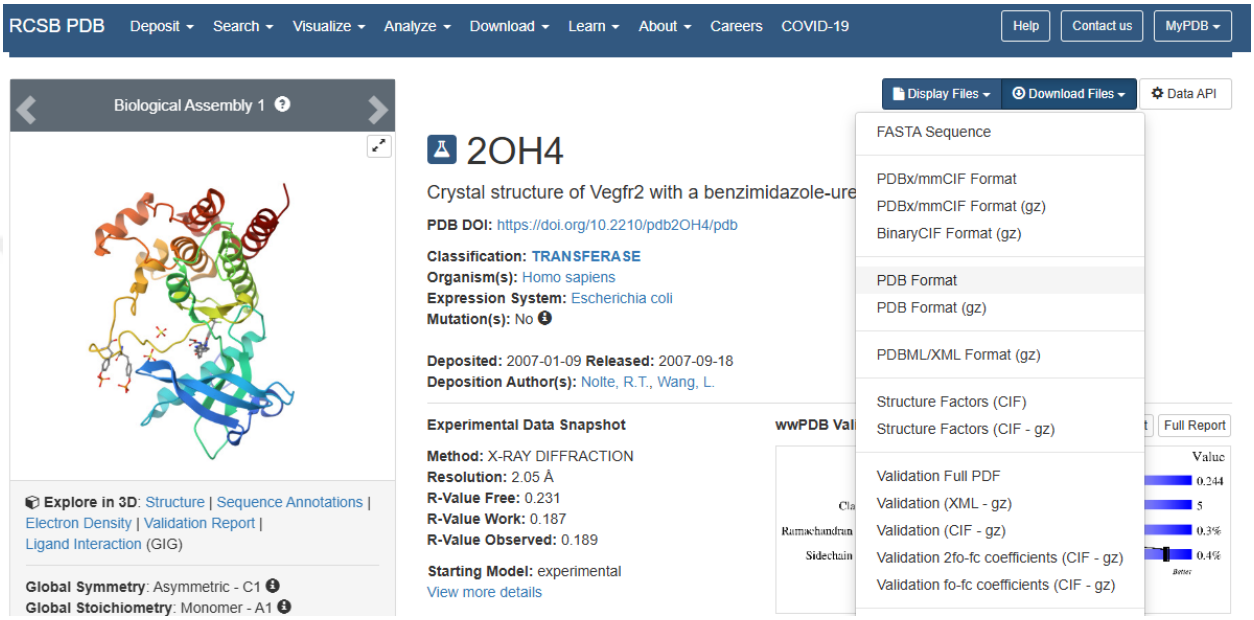


Figure 15. Downloading VEGFR2 (PDB ID: 2OH4) structure from the Protein Data Bank.

To optimize the protein for docking, the following steps were performed using Chimera:

- **Residue Removal:** Unwanted residues, such as water molecules and non-relevant ligands, were removed using the **Select** and **Action** menus, retaining only the main chain of the protein.
- **Docking Preparation:** The protein structure was prepared using the **Dock Prep** tool in Chimera (Figure 15). During this process:
    - Hydrogen atoms were added to the protein to ensure accurate representation of polar interactions.
    - The protein's net charge was adjusted to 0 to neutralize the structure.

- **Output File:** The optimized protein structure was saved in PDB format under the name "VEGFR2_prepared.pdb" for use in the docking analysis.

These preparation steps ensure the accuracy and reliability of the docking simulations by eliminating extraneous elements and stabilizing the protein structure for interaction studies.

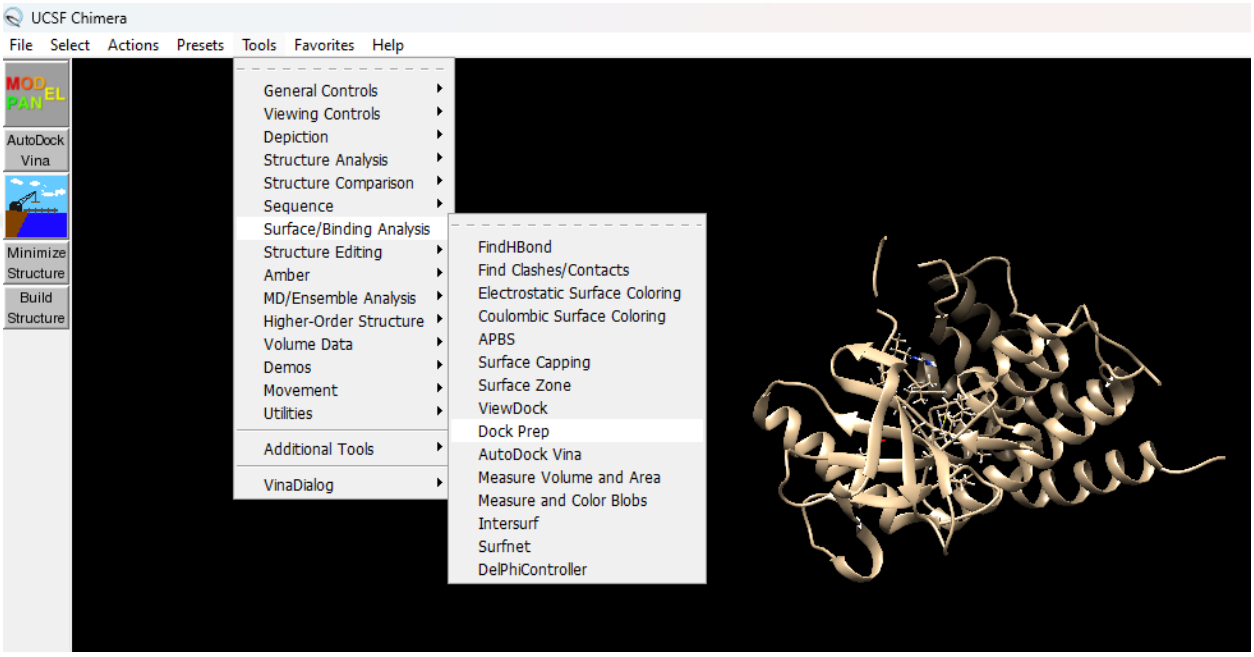


Figure 16. Docking Preparation: VEGFR2 protein structure was prepared using the Dock Prep tool in Chimera.

B. Molecule Preparation

Each compound identified from *E. spectabilis* was retrieved in canonical SMILES format from PubChem, except for 7,10′-bichrysophanol and chrysalodin, whose SMILES notations were manually generated in ChemDraw based on publication images.

- **Loading and Building the Structure:**
    - The canonical SMILES format was imported into Chimera through the **Structure Editing** menu under the "Build Structure" tab.

- **Structure Minimization:**
    - The molecular structure was minimized using the **Tools** menu in Chimera to optimize its geometry for docking (Figure 16).
- **Charge Assignment and Residue Naming:**
    - A neutral charge of +0 was applied to each molecule.
    - Each molecule was given a unique residue name for identification during docking.
- **File Saving:**
    - After preparation, the molecule was saved in MOL2 format, ready for docking analysis with VEGFR2.

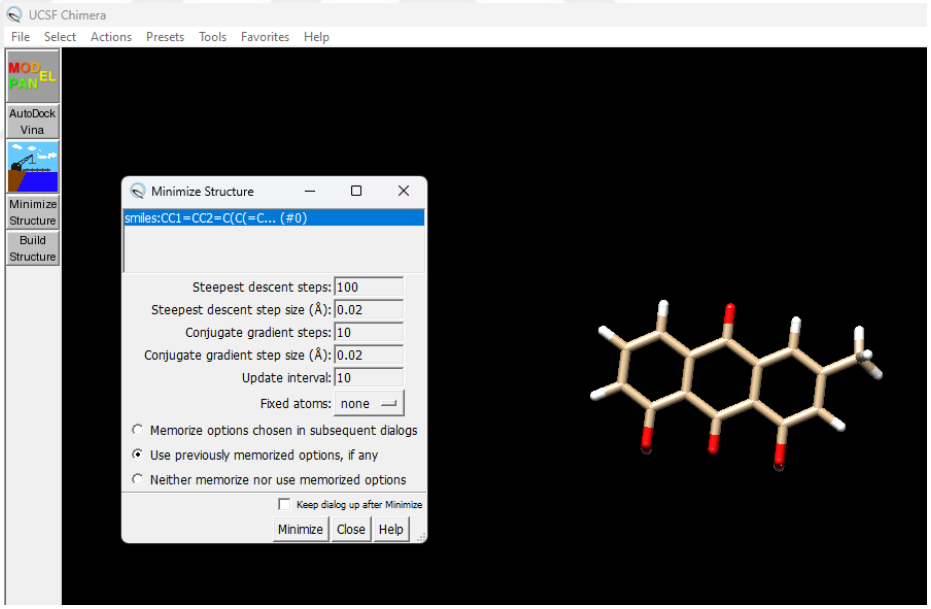


Figure 17. Structure Minimization step.

C. Grid Map Determination:

Docking was performed using a grid map to target the active binding site of VEGFR2. This grid map was generated based on the inhibitory ligand binding site in the enzyme to

examine potential binding interactions (Figure 17). The following parameters were used to generate the grid map:

- **Grid Dimensions:** 20 × 28 × 23 Å (size_x, size_y, size_z).
- **Grid Center:** 3, 34, and 17 Å (center_x, center_y, center_z).

AutoDock Vina was then employed to calculate the binding poses and energies for each compound.

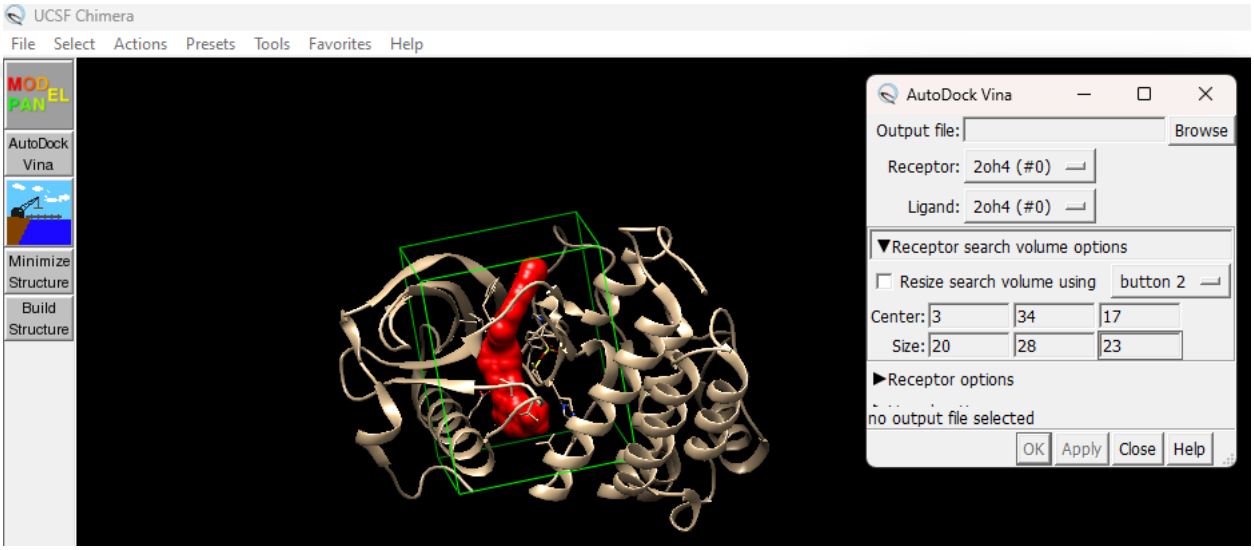


Figure 18. Grid Map Determination on VEGFR2 (2OH4).

D. Docking stimulation Using AutoDock Vina

The prepared enzyme (VEGFR2_prepared.pdb) and each molecule (in MOL2 format) were loaded into AutoDock Vina. After setting the grid map parameters around the active site, the files were converted to PDBQT format using AutoDock Tools and uploaded to AutoDock Vina for docking. The docking results, including binding poses and energies, were analyzed to identify the most favorable interactions for further study.

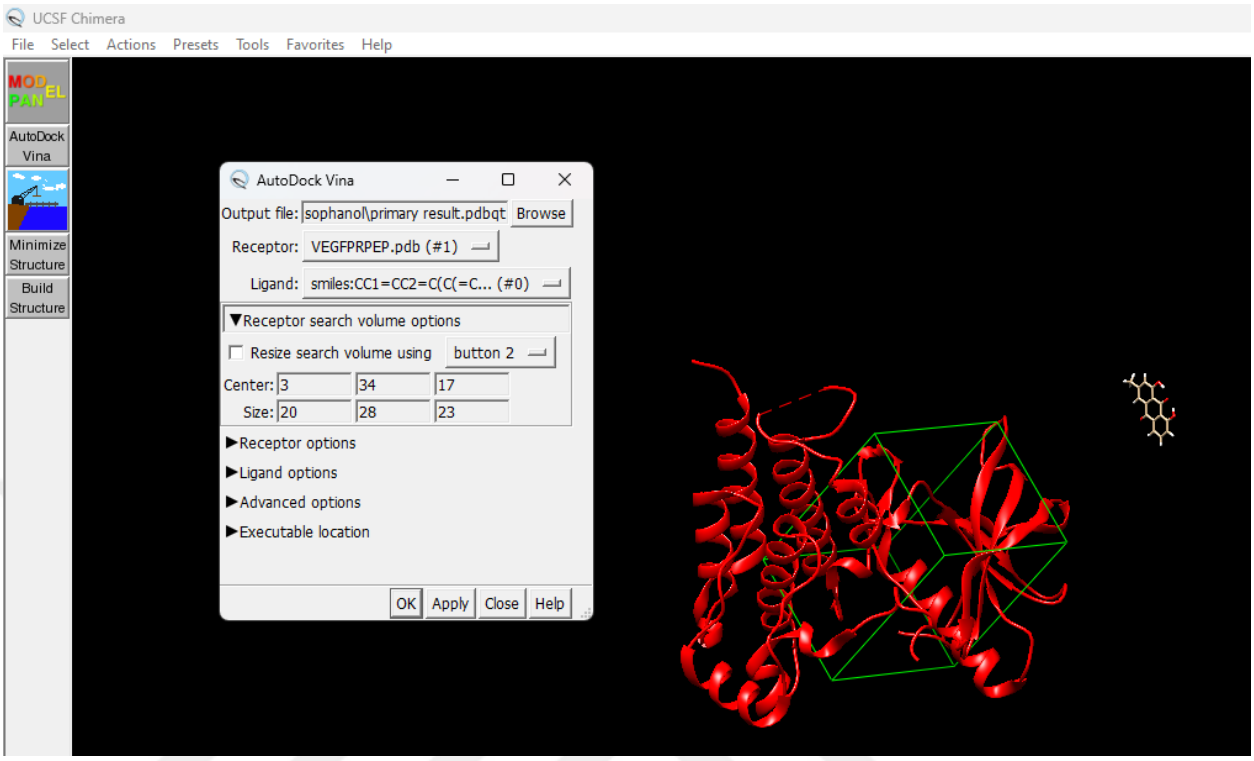


Figure 19. Docking stimulation Using AutoDock Vina.

Docking results included the binding energies and interaction poses of the *E. spectabilis* compounds with VEGFR2. The top poses with the lowest binding energies and RMSD values ≤ 2 Å were selected for further evaluation. Interaction details, including hydrogen bonds and binding residues, were analyzed using the PLIP server. This analysis provided insights into the molecular interactions, highlighting the compounds' potential as VEGFR2 inhibitors.

5.5. Statistical Analysis

Cytotoxicity assay results were obtained using Xcelligence RTCA Software Pro and GraphPad Prism 5.0 software.

6. RESULTS

6.1. Cytotoxicity of *E. spectabilis* Fractions on Hep3B Cells

In our study, different fractions of *E. spectabilis* were screened for cytotoxicity, aiming to investigate the cytotoxicity on the Hep3B cell line and to identify the most potent fractions that exhibit the most significant antiproliferative effects.

Following the culturing of Hep3B cells on an E-plate and a 24-hour incubation, diverse concentrations of the ES fractions (100, 50, and 10 µg/ml) were applied for variable durations (24, 48, and 72 hours) to evaluate their impact on cellular viability.

According to our findings, all fractions exhibited dose-dependent suppression of cell growth in Hep3B cells. Of the fractions analyzed, the ethyl acetate (ESEA) and aqueous ethanol (ESAE) fractions showed more efficacy than the chloroform (ESC) and hexane (ESH) fractions. The IC_{50} values for ESEA were measured at 6.53 µg/mL, 5.80 µg/mL, and 5.79 µg/mL for 24, 48, and 72 hours, respectively. The IC_{50} values for ESAE were 7.89 µg/mL, 5.40 µg/mL, and 5.37 µg/mL, and for ESC they were 23.15 µg/mL, 13.70 µg/mL, and 13.92 µg/mL, all measured at the same time points.

The ESH demonstrated the least activity, with IC_{50} values of 148.50 µg/mL, 40.73 µg/mL, and 8542.95 µg/mL over the same durations, indicating a lower potency compared to other fractions.

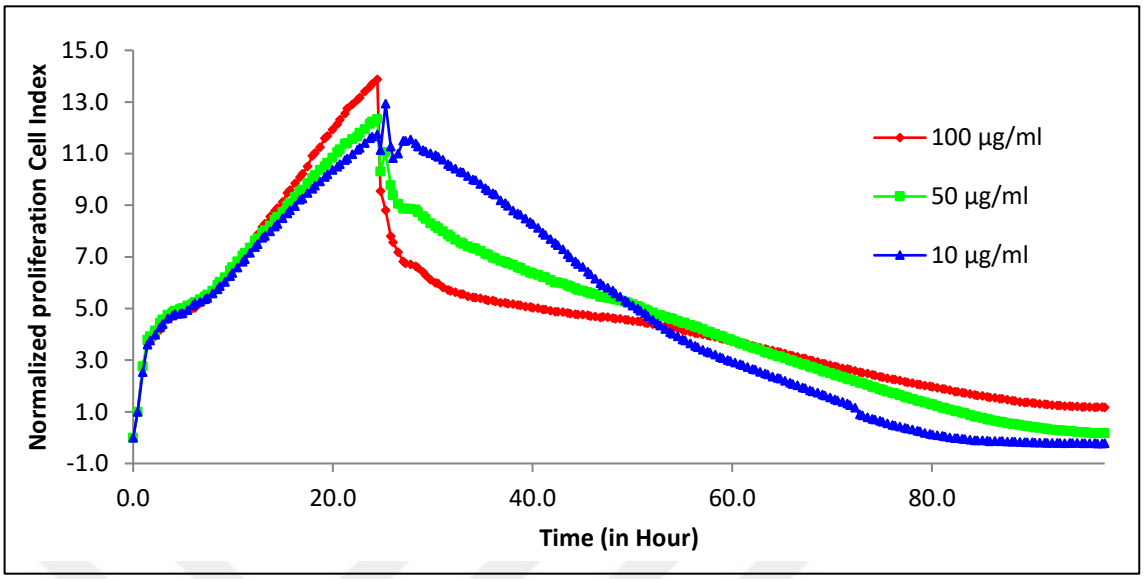


Figure 20. The effect of ESH fraction treated with different concentrations at various time intervals on Hep3B cells.

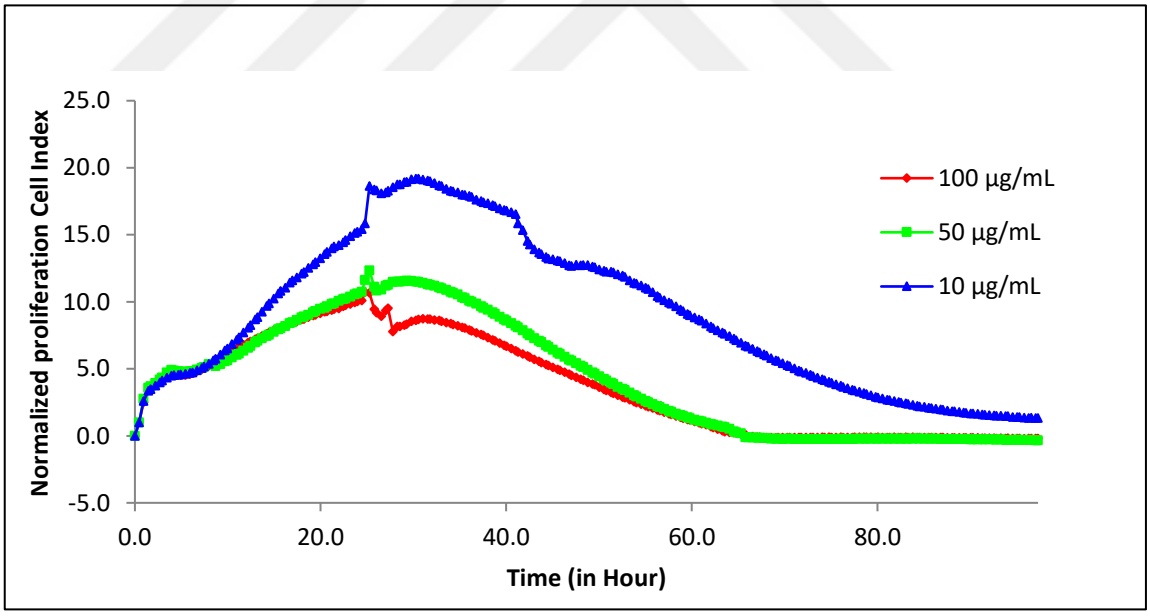


Figure 21. The effect of ESC fraction treated with different concentrations at various time intervals on Hep3B cells.

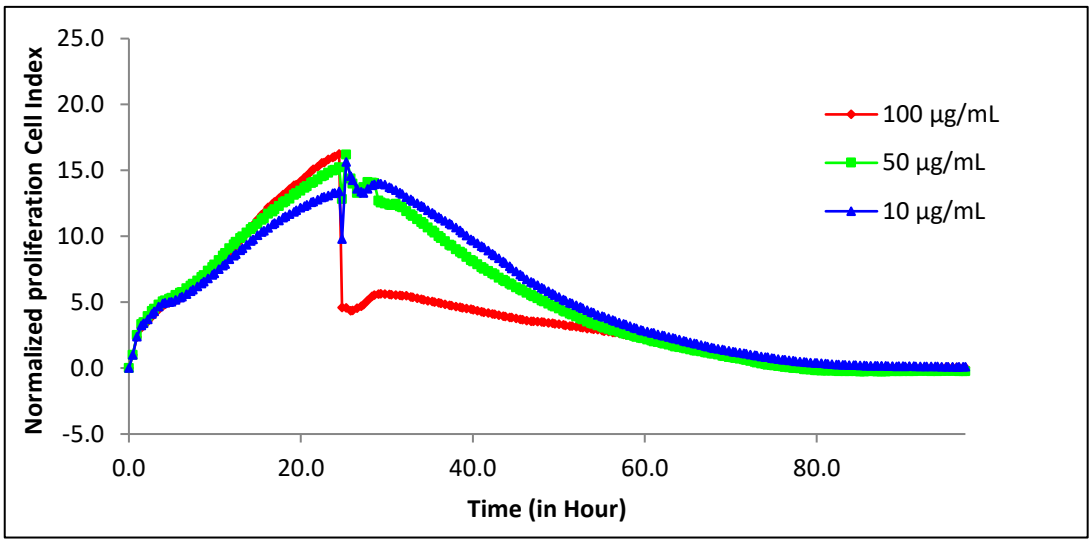


Figure 22. The effect of ESEA fraction treated with different concentrations at various time intervals on Hep3B cells.

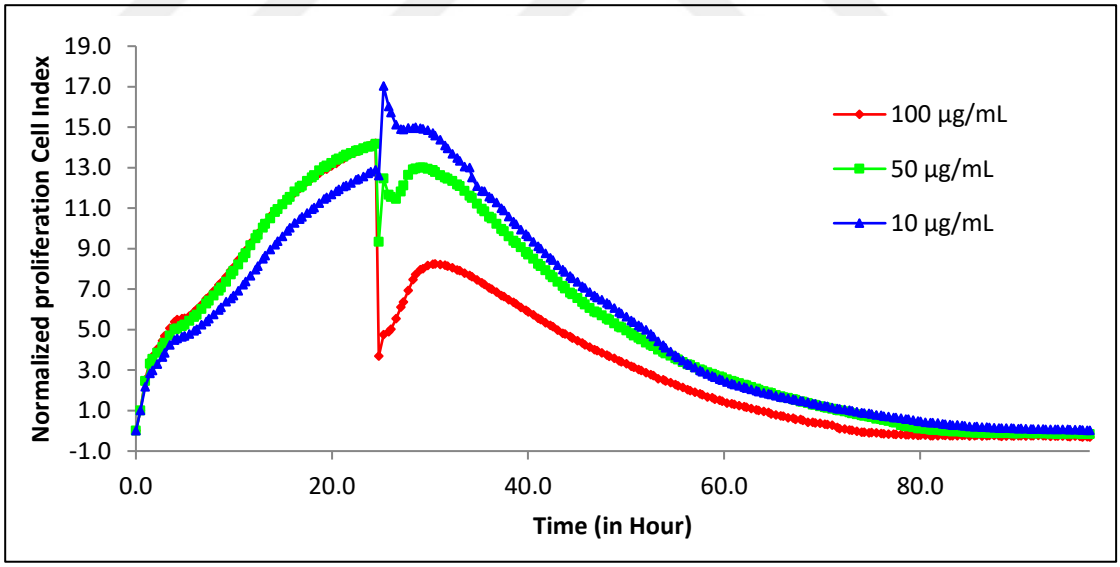


Figure 23. The effect of ESAE fraction treated with different concentrations at various time intervals on Hep3B cells.

6.2. Anti-Angiogenic Activity of *E. spectabilis* Fractions

Based on the analysis of *E. spectabilis* fractions for total vessel length, branching count, and total vessel area, the findings revealed a pronounced and robust anti-angiogenic effect at the IC_{50} and $IC_{50/2}$ concentrations (23.15 µg/mL and 11.57 µg/mL, respectively) of the ESC in comparison to the control (Figure 27). Moreover, ESH and ESEA had significant anti-angiogenic action at their IC_{50} concentrations (148.40 µg/mL and 6.53 µg/mL, respectively) but displayed weak effects at the $IC_{50/2}$ dose. Conversely, ESAE demonstrated limited anti-angiogenic effects at both the IC_{50} and $IC_{50/2}$ dosages.

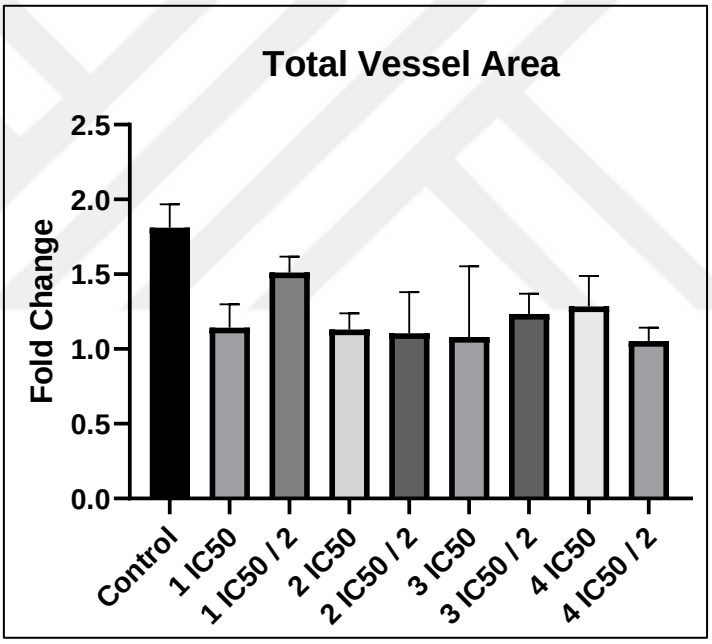


Figure 24. The fold change in total vessel area for each ES fraction after 24 hours. 1: ESH, 2: ESC, 3: ESEA, and 4: ESAE.

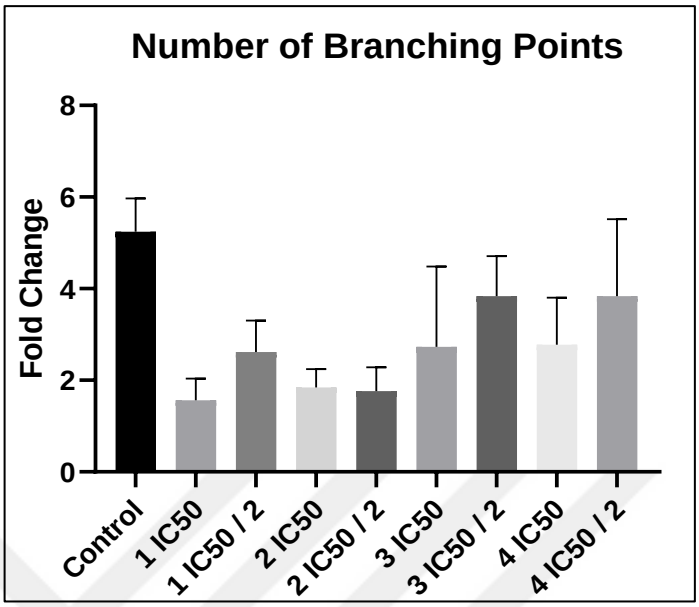


Figure 25. The fold change in branching points number for each ES fraction after 24 hours. 1: ESH, 2: ESC, 3: ESEA, and 4: ESAE.

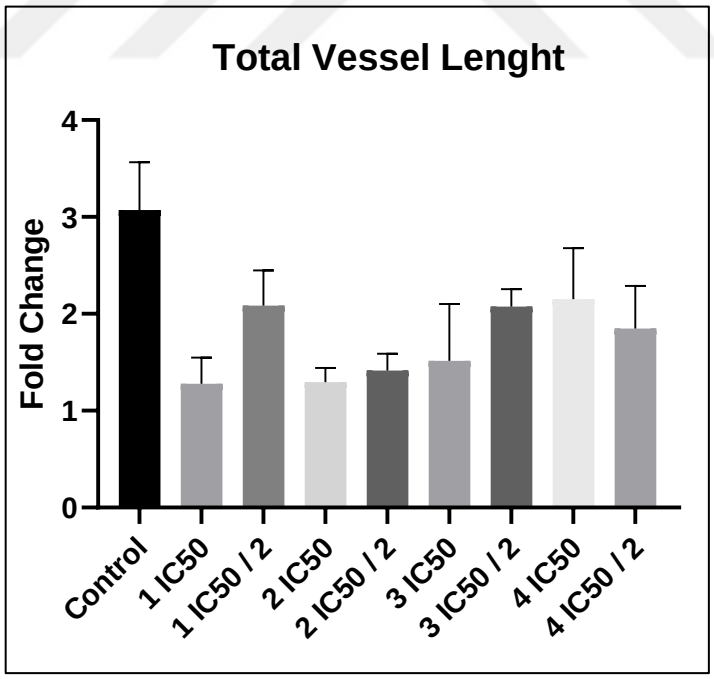


Figure 26. The fold change in total vessel length for each ES fraction after 24 hours. 1: ESH, 2: ESC, 3: ESEA, and 4: ESAE.

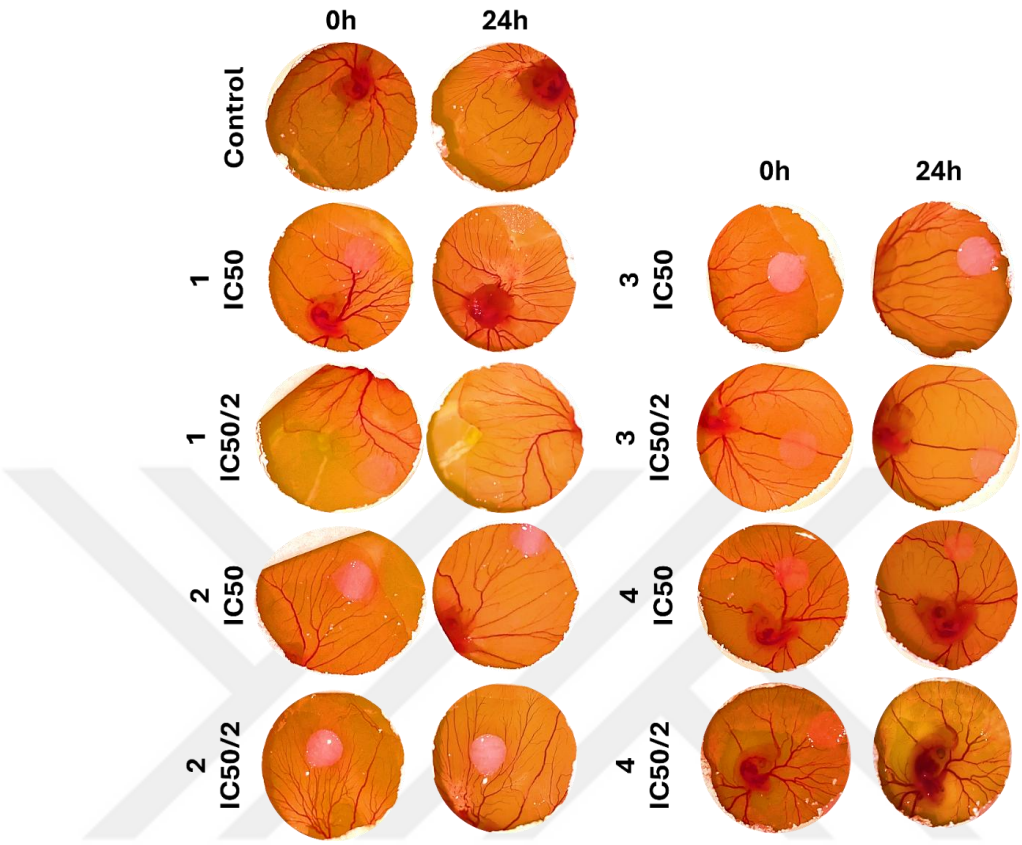


Figure 27. Inhibition of the capillaries on the CAM by ES fractions 1: ESH, 2: ESC, 3: ESEA, and 4: ESAE in both Ic_{50} and $Ic_{50/2}$ doses compared to control after 24 hours.



Figure 28. Illustration of capillary inhibition on the CAM by the ESC fraction at IC_{50} and $IC_{50/2}$ doses compared to the control after 24 hours.

6.3. Molecular Docking Results

Molecular docking analyses were performed on previously obtained chemicals from *E. spectabilis*. In the evaluation of VEGF-2 enzyme inhibition, almost all of the tested *E. spectabilis* phytochemicals exhibited significant and strong interactions, particularly 7,10′-bichrysophanol and chrysalodin. 7,10′-bichrysophanol achieved an impressive binding score of -10.8 kcal/mol compared to the control agents, Bacizumab and Apatinib, as evidenced by the data (Figure 28; Table 1). The interaction coordinates between the 7,10′-bichrysophanol molecule and the VEGF-2 enzyme (A chain) are X: 2.15446, Y: 25.0933, and Z: 18.6069. Similarly, chrysalodin exhibited a strong binding, obtaining a score of -10.7 kcal/mol, which is also higher than the binding score of the tested control agents. Moreover, chrysophanol revealed a good inhibitory binding to VEGFR2, with a score of -9.4 kcal/mol (Table 1).

Table 1. Docking Results: Binding Scores, Hydrogen Bonds, and Hydrophobic Interactions Number of Various ES Compounds (Control Compounds *).

compounds name	Binding score	Hydrophobic bonds no.	Hydrogen bonds no.
7,10′bichrysophanol	-10.8	8	5
Chrysalodin	-10.7	9	6
Chrysophanol	-9.4	5	4
Aloe emodin	-8.9	5	4
Isoorientin	-8.7	5	4
Daucosterol	-8.6	15	1
Inosine	-6.7	0	11
Bacizumab*	-8.3	8	2
Apatinib*	-9.5	12	1



Figure 29. The binding pose of 7,10′-bichrysophanol with VEGF-2, displaying a binding energy of -10.8 kcal/mol.



Figure 30. The binding pose of chrysalodin with VEGF-2, displaying a binding energy of -10.7 kcal/mol.

- **7,10′-Bichrysophanol: Binding Characteristics**

The lengths and angles of the possible hydrophobic and hydrogen bonds between the VEGF-2 enzyme and 7,10′-bichrysophanol were modeled, as shown below.

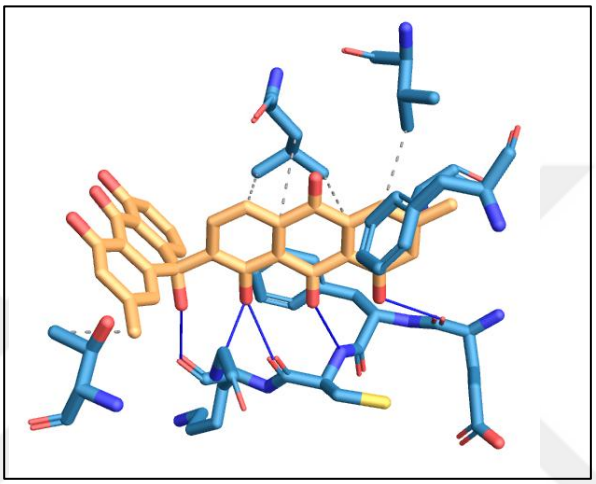


Figure 31. 7,10′-Bichrysophanol–VEGF-2 binding (-10.8 kcal/mol).

Table 2. Assessment of hydrophobic bonds between VEGF-2 and 7,10- bichrysophanol.

Index	Residue	AA	Distance	Ligand Atom	Protein Atom
1	838A	LEU	3.85	2406	214
2	838A	LEU	3.81	2407	211
3	838A	LEU	4.00	2411	213
4	846A	VAL	3.67	2412	268
5	864A	ALA	3.33	2416	399
6	916A	PHE	3.46	2398	795
7	924A	THR	3.52	2387	854
8	1045A	PHE	3.39	2412	1389

Table 3. Assessment of hydrogen bonds between VEGF-2 and 7,10′-bichrysophanol.

Index	Residue	AA	Distance H-A	Distance D-A	Donor Angle	Protein donor?	Side chain	Donor Atom	Acceptor Atom
1	915A	GLU	2.10	3.00	160.83	×	×	2421 [O3]	779 [O2]
2	917A	CYS	1.96	2.59	122.14	×	×	2422 [O3]	799 [O2]
3	917A	CYS	2.28	3.17	150.00	✓	×	796 [Nam]	2419 [O2]
4	918A	LYS	2.57	2.93	102.04	×	×	2403 [O3]	805 [O2]
5	920A	GLY	3.01	3.40	105.30	✓	×	822 [Nam]	2422 [O3]

- **Chrysalodin: Binding Characteristics**

The lengths and angles of the possible hydrophobic and hydrogen bonds between the VEGF-2 enzyme and chrysalodin were modeled, as shown below.

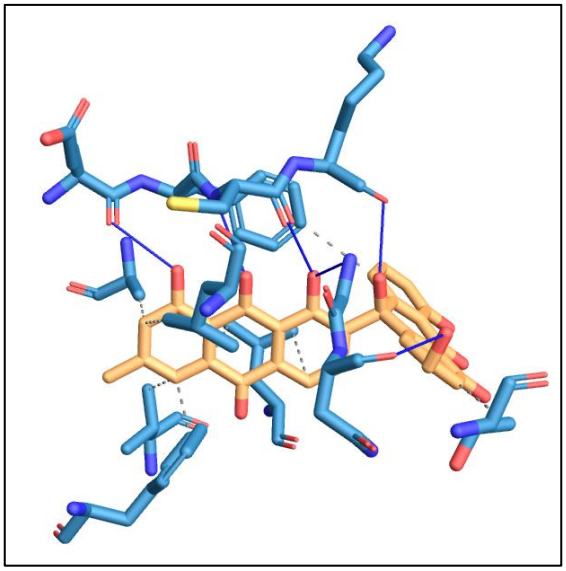


Figure 32. Chrysaoldin–VEGF-2 binding (-10.7 kcal/mol).

Table 4. Assessment of hydrophobic bonds between VEGF-2 and chrysalodin.

Index	Residue	AA	Distance	Ligand Atom	Protein Atom
1	838A	LEU	3.93	2417	214
2	838A	LEU	3.86	2406	211
3	838A	LEU	4.00	2410	213
4	846A	VAL	3.66	2414	268
5	864A	ALA	3.29	2411	399
6	916A	PHE	3.54	2389	795
7	924A	THR	3.84	2398	854
8	1033A	LEU	3.97	2411	1294
9	1045A	PHE	3.39	2414	1389

Table 5. Assessment of hydrogen bonds between VEGF-2 and chrysalodin.

Index	Residue	AA	Distance H-A	Distance D-A	Donor Angle	Protein donor?	Side chain	Donor Atom	Acceptor Atom
1	915A	GLU	2.12	3.02	162.32	×	×	2420 [O3]	779 [O2]
2	917A	CYS	1.94	2.59	124.97	×	×	2419 [O3]	799 [O2]
3	917A	CYS	2.28	3.17	150.48	✓	×	796 [Nam]	2408 [O2]
4	918A	LYS	2.59	2.96	102.75	×	×	2421 [O3]	805 [O2]
5	920A	GLY	2.94	3.32	103.91	✓	×	822 [Nam]	2419 [O3]
6	921A	ASN	2.49	3.24	133.65	×	×	2425 [O3]	829 [O2]

7. DISCUSSION and CONCLUSION

Phytochemicals have demonstrated significant utility in the formulation of standardized cancer treatment methodologies. The initial instance was the chemotherapeutic agent Paclitaxel, known as Taxol, which was derived from the bark of Taxus brevifolia in 1971 and is utilized in medicinal contexts to inhibit cell multiplication (Bender & Atalay, 2018). Following the groundbreaking success of Paclitaxel, numerous other natural-derived compounds have demonstrated significant anticancer properties, and ongoing plant-based research continues to yield remarkable insights and promising results in the fight against cancer. In this context, the current study evaluates the cytotoxic effects of various *E. spectabilis* fractions—ESH, ESC, ESEA, and ESAE—on the Hep3B cell line using the xCELLigence® RTCA assay.

Plant extracts with IC_{50} values below 20–30 µg/mL are regarded as prospective anticancer agents, according to the American National Cancer Institute guidelines. In accordance with this criterion and our established methodology for assessing IC_{50} values at various concentrations, we utilized dosages of 10, 50, and 100 µg/mL in this work to examine the cytotoxic effects on Hep3B cells. The selected concentrations were intended to facilitate precise IC_{50} estimation, enabling the evaluation of the extracts' potential efficacy in preventing cancer cell proliferation (Boik, 2001; Canga et al., 2022). As a result of the current experiments, the fractions from *E. spectabilis* showed cytotoxic effects against HCC (Hep3B). The active concentrations identified generally align with the American NCI guidelines. The IC_{50} values for ESEA against the Hep3B cell line were 6.53, 5.80, and 5.79 µg/mL for 24, 48, and 72 hours, respectively. For ESAE, the IC_{50} values were 7.89, 5.40, and 5.37 µg/mL, while for ESC they were 23.15, 13.70, and 13.92 µg/mL, all measured at the same time points.

Anthraquinones, coumarins, terpenoids, and flavonoids were found in Eremurus species, according to previous research (Farhadi et al., 2023). Reportedly, anthraquinones, coumarins, terpenoids, and flavonoids have all shown promise as anticancer agents (Huang et al., 2012; Malik et al., 2021; Önder, 2020; Ren et al., 2003). Therefore, *E. spectabilis* might have an anticancer effect against Hep3B due to these classes of chemicals.

The anti-angiogenesis effect of *E. spectabilis* utilizing the CAM assay has never been discussed before in the literature until our investigation. At concentrations of IC_{50} and $IC_{50/2}$ µg/mL, ESC demonstrated strong and significant antiangiogenic effects on CAM, measured by total vessel length, branching count, and total vessel area. Anthraquinones (Fernand et al., 2011; Kaneshiro et al., 2006; Kwak et al., 2006; Vidal et al., 2023), coumarins (Majnooni et al., 2019), terpenoids (Kuttan et al., 2011; Lu et al., 2023), and flavonoids (Mirossay et al., 2017) are proposed to exhibit anti-angiogenic properties. Consequently, this secondary metabolic group present in *E. spectabilis* may account for the plant's activity.

Docking tests were performed to examine the anti-angiogenesis mechanism. To evaluate the interaction with the enzyme VEGFR-2, the phytochemical compounds that were identified from *E. spectabilis* in earlier studies were docked into its binding site (PDB ID: 2OH4).

The binding of VEGFA, B, C, or D triggers the expression of VEGFR2, which is expressed by nearly all ECs. The PI3K/AKT and RAF/MAPK pathways are two examples of downstream cellular signaling pathways that are activated when VEGFA binds to VEGFR2. This process leads to the proliferation and migration of ECs as well as the formation of new branches of blood vessels, which are crucial for the rapid growth and metastasis of tumors (Shaw et al., 2024; Yao et al., 2023). These findings emphasize the importance of targeting VEGFR-2 to decrease angiogenesis.

The comparative docking analysis between the well-known antiangiogenic drugs bevacizumab and atapatinib, both of which inhibit VEGFR-2, and the phytochemicals previously identified from *E. spectabilis* in earlier studies indicated that the phytochemicals extracted with chloroform yielded outcomes comparable to the controls. Notably, 7,10′-bichrysophanol (-10.8 kcal/mol) and chrysalodin (-10.7 kcal/mol) showed the highest binding scores, surpassing both control samples. This additionally suggests that the chloroform fraction of *E. spectabilis* may effectively inhibit new blood vessel formation.

All of these results indicate that the *E. spectabilis* fractions have inhibitory effects on hepatocellular carcinoma, particularly the ESEA and ESAE fractions with IC_{50} values that align with American guidelines. Furthermore, the ESC has the ability to diminish

angiogenesis in terms of total vessel length, branching count, and total vessel area, which indicates that it has the potential to be a good candidate for further exploration and development as an anti-cancer and anti-angiogenesis agent. It was also proven that most of the phytochemicals discovered from chloroform extract bind to the VEGFR-2 enzyme with extremely effective energy, suggesting great potential for inhibiting the VEGFR-2 enzyme.

Overall, this study suggests that ES is a dual-action option for cancer therapy. On the other hand, additional investigations are necessary with regard to the absolute configuration and the mechanism of action to confirm these results and explore them in depth.

8. REFERENCES

Asafo-Agyei, K. O., & Samant, H. (2023). Hepatocellular carcinoma. *StatPearls*. https://europepmc.org/books/n/statpearls/article-22805/?extid=30855838&src=med

Ataergin, A., Özet, A., & Arpacı, F. (1999). The place of angiogenesis inhibitors in cancer therapy. *Turk Klin J Med Sci*, *19*, 100-105.

Ayuso, C., Rimola, J., Vilana, R., Burrel, M., Darnell, A., García-Criado, Á., Bianchi, L., Belmonte, E., Caparroz, C., & Barrufet, M. (2018). Diagnosis and staging of hepatocellular carcinoma (HCC): current guidelines. *European Journal of Radiology*, *101*, 72-81. https://doi.org/10.1016/j.ejrad.2018.01.025

Baker, S. D., Sparreboom, A., & Verweij, J. (2006). Clinical pharmacokinetics of docetaxel: recent developments. *Clinical Pharmacokinetics*, *45*, 235-252.

Balunas, M. J., & Kinghorn, A. D. (2005). Drug discovery from medicinal plants. *Life Sciences*, *78*(5), 431-441. https://doi.org/10.1016/j.lfs.2005.09.012

Bayrak, B. B., & Yanardağ, R. (2021). Antioxidant Activities of Eremurus spectabilis M. Bieb. Extracts and Sulfur Compounds. *European Journal of Biology*, *80*(2), 154-163. https://doi.org/10.26650/EurJBiol.2021.1028656

Bender, O., & Atalay, A. (2018). Evaluation of anti-proliferative and cytotoxic effects of chlorogenic acid on breast cancer cell lines by real-time, label-free and high-throughput screening. *Marmara Pharmaceutical Journal*, *22*(2).

Berg, C. D., Schiller, J. H., Boffetta, P., Cai, J., Connolly, C., Kerpel-Fronius, A., Kitts, A. B., Lam, D. C., Mohan, A., & Myers, R. (2023). Air pollution and lung cancer: a review by International Association for the Study of Lung Cancer Early Detection and Screening Committee. *Journal of Thoracic Oncology*, *18*(10), 1277-1289. https://doi.org/10.1016/j.jtho.2023.05.024

BioRender. Alhalak, N. , (2024). Schematic representation Retrieved from https://app.biorender.com

Bizim Bitkiler. Çiriş (Eremurus) M.Bieb. Cent. Pl. Ross. Merid. 2: t. 61 (1832). (2024). https://bizimbitkiler.org.tr/v2/hiyerarsi.php?c=Eremurus

Boik, J. (2001). *Natural Compounds in Cancer Therapy*. Oregon Medical Press. https://www.cabidigitallibrary.org/doi/full/10.5555/20013083846

Canga, I., Vita, P., Oliveira, A. I., Castro, M. Á., & Pinho, C. (2022). In vitro cytotoxic activity of african plants: A review. *Molecules*, *27*(15), 4989. https://doi.org/10.3390/molecules27154989

Carmeliet, P., & Jain, R. K. (2000). Angiogenesis in cancer and other diseases. *Nature*, *407*(6801), 249-257.

Chatterjee, N., & Walker, G. C. (2017). Mechanisms of DNA damage, repair, and mutagenesis. *Environmental and Molecular Mutagenesis*, *58*(5), 235-263. https://doi.org/10.1002/em.22087

Distler, J., Hirth, A., Kurowska-Stolarska, M., & Gay, R. (2003). Angiogenic and angiostatic factors in the molecular control of angiogenesis. *The Quarterly Journal of Nuclear Medicine and Molecular Imaging*, *47*(3), 149.

Duan, B., Huang, C., Bai, J., Zhang, Y. L., Wang, X., Yang, J., & Li, J. (2019). Multidrug resistance in hepatocellular carcinoma. *Exon Publications*, 141-158. https://doi.org/10.15586/hepatocellularcarcinoma.2019.ch8

Engin, A. (2017). Non-alcoholic fatty liver disease. *Obesity and Lipotoxicity*, 443-467.

Farhadi, F., Avan, R., Sahebkar, A., & Eghbali, S. (2023). A comprehensive review on Eremurus species: phytochemistry, pharmacology and traditional uses. *Phytochemistry Letters*, *53*, 142-149. https://doi.org/10.1016/j.phytol.2022.12.002

Fernand, V. E., Losso, J. N., Truax, R. E., Villar, E. E., Bwambok, D. K., Fakayode, S. O., Lowry, M., & Warner, I. M. (2011). Rhein inhibits angiogenesis and the viability of hormone-dependent and-independent cancer cells under normoxic or hypoxic conditions in vitro. *Chemico-Biological Interactions*, *192*(3), 220-232. https://doi.org/10.1016/j.cbi.2011.03.013

Fernández-Palanca, P., Fondevila, F., Méndez-Blanco, C., Tuñón, M. J., González-Gallego, J., & Mauriz, J. L. (2019). Antitumor effects of quercetin in hepatocarcinoma in vitro and in vivo models: a systematic review. *Nutrients*, *11*(12), 2875. https://doi.org/10.3390/nu11122875

Grundy, S. M. (2004). Obesity, metabolic syndrome, and cardiovascular disease. *The Journal of Clinical Endocrinology & Metabolism*, *89*(6), 2595-2600. https://doi.org/10.1210/jc.2004-0372

Hamzawy, M. A., El-Denshary, E. S., & Abdel-Wahhab, M. A. (2015). Effects of natural compounds in treatment and prevention of hepatotoxicity and hepatocellular carcinoma. *Hepatoma Research*, *1*, 111-118.

Hanahan, D., & Weinberg, R. A. (2011). Hallmarks of cancer: the next generation. *Cell*, *144*(5), 646-674.

Hoenerhoff, M. J., Boyle, M., Minocherhomji, S., & Pandiri, A. R. (2022). Carcinogenesis: mechanisms and evaluation. In *Haschek and Rousseaux's Handbook of Toxicologic*

Pathology (pp. 205-254). Elsevier. https://doi.org/10.1016/B978-0-12-821044-4.00013-3

Huang, M., Lu, J.-J., Huang, M.-Q., Bao, J.-L., Chen, X.-P., & Wang, Y.-T. (2012). Terpenoids: natural products for cancer therapy. *Expert Opinion on Investigational Drugs*, *21*(12), 1801-1818. https://doi.org/10.1517/13543784.2012.727395

Iruela-Arispe, L. M., & Dvorak, H. F. (1997). Angiogenesis: a dynamic balance of stimulators and inhibitors. *Thrombosis and Haemostasis*, *78*(07), 672-677. https://doi.org/10.1055/s-0038-1657610

Jahanbin, K., Abbasian, A., & Ahang, M. (2017). Isolation, purification and structural characterization of a new water-soluble polysaccharide from Eremurus stenophyllus (boiss. & buhse) baker roots. *Carbohydrate Polymers*, *178*, 386-393. https://doi.org/10.1016/j.carbpol.2017.09.058

Jamshidi-Parsian, A., Griffin, R. J., Kore, R. A., Todorova, V. K., & Makhoul, I. (2018). Tumor-endothelial cell interaction in an experimental model of human hepatocellular carcinoma. *Experimental Cell Research*, *372*(1), 16-24. https://doi.org/10.1016/j.yexcr.2018.09.001

Ján, T., Dáša, S., Igor, A., & Jana, V. (2020). Systemic treatment for hepatocellular carcinoma. *Klinicka Onkologie: Casopis Ceske a Slovenske Onkologicke Spolecnosti*, *33*(5), 356-361. https://doi.org/10.14735/amko2020356

Jemal, A., Ward, E. M., Johnson, C. J., Cronin, K. A., Ma, J., Ryerson, A. B., Mariotto, A., Lake, A. J., Wilson, R., & Sherman, R. L. (2017). Annual report to the nation on the status of cancer, 1975–2014, featuring survival. *JNCI: Journal of the National Cancer Institute*, *109*(9), djx030. https://doi.org/10.1093/jnci/djx030

Kaneshiro, T., Morioka, T., Inamine, M., Kinjo, T., Arakaki, J., Chiba, I., Sunagawa, N., Suzui, M., & Yoshimi, N. (2006). Anthraquinone derivative emodin inhibits tumor-associated angiogenesis through inhibition of extracellular signal-regulated kinase 1/2 phosphorylation. *European Journal of Pharmacology*, *553*(1-3), 46-53. https://doi.org/10.1016/j.ejphar.2006.09.026

Karakaya, L., Akgül, Y., & Nalbantsoy, A. (2017). Chemical constituents and in vitro biological activities of Eremurus spectabilis leaves. *Natural Product Research*, *31*(15), 1786-1791. https://doi.org/10.1080/14786419.2017.1292268

Kenmotsu, H., & Tanigawara, Y. (2015). Pharmacokinetics, dynamics and toxicity of docetaxel: Why the Japanese dose differs from the Western dose. *Cancer Science*, *106*(5), 497-504. https://doi.org/10.1111/cas.12647

Koldas, S. (2023). Absolute configurations of biantraquinones from Eremurus spectabilis BIEB. *Natural Product Research*, 1-9. https://doi.org/10.1080/14786419.2023.2272779

Konukoğlu, D., & Turhan, S. (2005). Molecular basis of angiogenesis mechanisms and tumor angiogenesis. *Cerrahpaşa J Med*, *36*, 42-48.

Koya, A. I., & Ibrahim, S. A. (2024). Carcinogenesis. *StatPearls*. https://pubmed.ncbi.nlm.nih.gov/38917272/

Kuttan, G., Pratheeshkumar, P., Manu, K. A., & Kuttan, R. (2011). Inhibition of tumor progression by naturally occurring terpenoids. *Pharmaceutical Biology*, *49*(10), 995-1007. https://doi.org/10.3109/13880209.2011.559476

Kwak, H. J., Park, M. J., Park, C. M., Moon, S. I., Yoo, D. H., Lee, H. C., Lee, S. H., Kim, M. S., Lee, H. W., & Shin, W. S. (2006). Emodin inhibits vascular endothelial growth factor-A-induced angiogenesis by blocking receptor-2 (KDR/Flk-1) phosphorylation. *International Journal of Cancer*, *118*(11), 2711-2720. https://doi.org/10.1002/ijc.21641

Llovet, J. M., Brú, C., & Bruix, J. (1999). Prognosis of hepatocellular carcinoma: the BCLC staging classification. *Seminars in Liver Disease*, *19*(03), 329-338. https://doi.org/10.1055/s-2007-1007122

Llovet, J. M., Zucman-Rossi, J., Pikarsky, E., Sangro, B., Schwartz, M., Sherman, M., & Gores, G. (2016). Hepatocellular carcinoma. *Nature Reviews. Disease primers*, *2*, 16018-16018. https://doi.org/10.1038/nrdp.2016.18

Lok, A. S., Seeff, L. B., Morgan, T. R., Di Bisceglie, A. M., Sterling, R. K., Curto, T. M., Everson, G. T., Lindsay, K. L., Lee, W. M., & Bonkovsky, H. L. (2009). Incidence of hepatocellular carcinoma and associated risk factors in hepatitis C-related advanced liver disease. *Gastroenterology*, *136*(1), 138-148. https://doi.org/10.1053/j.gastro.2008.09.014

Lu, X., Friedrich, L. J., & Efferth, T. (2023). Natural products targeting tumour angiogenesis. *British Journal of Pharmacology*. https://doi.org/10.1111/bph.16232

Majnooni, M. B., Fakhri, S., Smeriglio, A., Trombetta, D., Croley, C. R., Bhattacharyya, P., Sobarzo-Sánchez, E., Farzaei, M. H., & Bishayee, A. (2019). Antiangiogenic effects of coumarins against cancer: From chemistry to medicine. *Molecules*, *24*(23), 4278. https://doi.org/10.3390/molecules24234278

Malik, M. S., Alsantali, R. I., Jassas, R. S., Alsimaree, A. A., Syed, R., Alsharif, M. A., Kalpana, K., Morad, M., Althagafi, I. I., & Ahmed, S. A. (2021). Journey of anthraquinones as anticancer agents–a systematic review of recent literature. *RSC Advances*, *11*(57), 35806-35827. https://doi.org/10.1039/D1RA05686G

Marin, J. J., Macias, R. I., Monte, M. J., Romero, M. R., Asensio, M., Sanchez-Martin, A., Cives-Losada, C., Temprano, A. G., Espinosa-Escudero, R., & Reviejo, M. (2020). Molecular bases of drug resistance in hepatocellular carcinoma. *Cancers*, *12*(6), 1663. https://doi.org/10.3390/cancers12061663

Massarweh, N. N., & El-Serag, H. B. (2017). Epidemiology of hepatocellular carcinoma and intrahepatic cholangiocarcinoma. *Cancer Control*, *24*(3), 1073274817729245. https://doi.org/10.1177/1073274817729245

McGlynn, K. A., Petrick, J. L., & London, W. T. (2015). Global epidemiology of hepatocellular carcinoma: an emphasis on demographic and regional variability. *Clinics in Liver Disease*, *19*(2), 223-238.

Mirossay, L., Varinská, L., & Mojžiš, J. (2017). Antiangiogenic effect of flavonoids and chalcones: An update. *International Journal of Molecular Sciences*, *19*(1), 27. https://doi.org/10.3390/ijms19010027

Mohammed, I. F., & Kaka, L. N. (2007). Promotion of regenerative processes in injured peripheral nerve induced by low-level laser therapy. *Photomedicine and Laser Surgery*, *25*(2), 107-111. https://doi.org/10.1089/pho.2006.1090

Montero, A., Fossella, F., Hortobagyi, G., & Valero, V. (2005). Docetaxel for treatment of solid tumours: a systematic review of clinical data. *The Lancet Oncology*, *6*(4), 229-239.

Motofei, I. G. (2022). Biology of cancer; from cellular and molecular mechanisms to developmental processes and adaptation. *Seminars in Cancer Biology, 86*, 600-615. https://doi.org/10.1016/j.semcancer.2021.10.003

Nash, K. L., Woodall, T., Brown, A. S., Davies, S. E., & Alexander, G. J. (2010). Hepatocellular carcinoma in patients with chronic hepatitis C virus infection without cirrhosis. *World Journal of Gastroenterology: WJG*, *16*(32), 4061. https://doi.org/10.3748/wjg.v16.i32.4061

Önder, A. (2020). Anticancer activity of natural coumarins for biological targets. *Studies in Natural Products Chemistry, 64*, 85-109. https://doi.org/10.1016/B978-0-12-817903-1.00003-6

Paper, D. H. (1998). Natural products as angiogenesis inhibitors. *Planta Medica*, *64*(8), 686–695.

Polverini, P. J. (1995). The pathophysiology of angiogenesis. *Critical Reviews in Oral Biology & Medicine*, *6*(3), 230-247. https://doi.org/10.1177/10454411950060030501

Pubchem. (2024). Compound Summary for Eremurus spectabilis phytochemicals. https://pubchem.ncbi.nlm.nih.gov/

Rajabi, M., & Mousa, S. A. (2017). The role of angiogenesis in cancer treatment. *Biomedicines*, *5*(2), 34. https://doi.org/10.3390/biomedicines5020034

Ren, W., Qiao, Z., Wang, H., Zhu, L., & Zhang, L. (2003). Flavonoids: promising anticancer agents. *Medicinal Research Reviews*, *23*(4), 519-534. https://doi.org/10.1002/med.10033

Rezzola, S., Loda, A., Corsini, M., Semeraro, F., Annese, T., Presta, M., & Ribatti, D. (2020). Angiogenesis-inflammation cross talk in diabetic retinopathy: novel insights from the chick embryo chorioallantoic membrane/human vitreous platform. *Frontiers in Immunology*, *11*, 581288. https://doi.org/10.3389/fimmu.2020.581288

Ribatti, D. (2008). *History of research on tumor angiogenesis*. Springer Science & Business Media. https://doi.org/10.1007/978-1-4020-9563-4

Ribatti, D. (2017). The chick embryo chorioallantoic membrane (CAM) assay. *Reproductive Toxicology*, *70*, 97-101. https://doi.org/10.1016/j.reprotox.2016.11.004

Ribatti, D., Annese, T., Ruggieri, S., Tamma, R., & Crivellato, E. (2019). Limitations of anti-angiogenic treatment of tumors. *Translational Oncology*, *12*(7), 981-986. https://doi.org/10.1016/j.tranon.2019.04.022

Sanyal, A. J., Yoon, S. K., & Lencioni, R. (2010). The etiology of hepatocellular carcinoma and consequences for treatment. *The Oncologist*, *15*(S4), 14-22. https://doi.org/10.1634/theoncologist.2010-S4-14

Schulze, K., Nault, J.-C., & Villanueva, A. (2016). Genetic profiling of hepatocellular carcinoma using next-generation sequencing. *Journal of Hepatology*, *65*(5), 1031-1042. https://doi.org/10.1016/j.jhep.2016.05.035

Seca, A. M., & Pinto, D. C. (2018). Plant secondary metabolites as anticancer agents: successes in clinical trials and therapeutic application. *International Journal of Molecular Sciences*, *19*(1), 263. https://doi.org/10.3390/ijms19010263

Semela, D., & Dufour, J.-F. (2004). Angiogenesis and hepatocellular carcinoma. *Journal of Hepatology*, *41*(5), 864-880. https://doi.org/10.1016/j.jhep.2004.09.006

Shaw, P., Dwivedi, S. K. D., Bhattacharya, R., Mukherjee, P., & Rao, G. (2024). VEGF signaling: Role in angiogenesis and beyond. *Biochimica et Biophysica Acta (BBA)-Reviews on Cancer*, 189079. https://doi.org/10.1016/j.bbcan.2024.189079

Singal, A. G., Llovet, J. M., Yarchoan, M., Mehta, N., Heimbach, J. K., Dawson, L. A., Jou, J. H., Kulik, L. M., Agopian, V. G., & Marrero, J. A. (2023). AASLD practice guidance on prevention, diagnosis, and treatment of hepatocellular carcinoma. *Hepatology*, *78*(6), 1922-1965. https://doi.org/10.1097/HEP.0000000000000466

Singh, A. K., Kumar, R., & Pandey, A. K. (2018). Hepatocellular carcinoma: causes, mechanism of progression and biomarkers. *Current Chemical Genomics and Translational Medicine*, *12*, 9. https://doi.org/10.2174/2213988501812010009

Sugawara, Y., & Hibi, T. (2022). Liver transplantation for patients with hepatocellular carcinoma: Its current status and advances. *Bioscience Trends*, *16*(3), 207-211. https://doi.org/10.5582/bst.2022.01199

Suresh, D., Srinivas, A. N., & Kumar, D. P. (2020). Etiology of hepatocellular carcinoma: special focus on fatty liver disease. *Frontiers in Oncology*, *10*, 601710. https://doi.org/10.3389/fonc.2020.601710

Syn, N. L. X., Wang, L., Wong, A. L. A., Soe, M. Y., Chuah, B., Chan, D., Tan, S. H., Soo, R. A., Lee, S. C., & Goh, B. C. (2016). Dose modifications in Asian cancer patients with hepatic dysfunction receiving weekly docetaxel: A prospective pharmacokinetic and safety study. *Cancer Science*, *107*(2), 173-180. https://doi.org/10.1111/cas.12856

Taskin, T., Bitis, L., & Birteksöz, S. (2012). Antioxidant and antimicrobial activities of different extracts from Eremurus spectabilis leaves. *Spatula DD-Peer Reviewed Journal on Complementary Medicine and Drug Discovery*, *2*(4), 213.

Tellapuri, S., Sutphin, P. D., Beg, M. S., Singal, A. G., & Kalva, S. P. (2018). Staging systems of hepatocellular carcinoma: a review. *Indian Journal of Gastroenterology*, *37*, 481-491.

Testino, G., Leone, S., & Borro, P. (2014). Alcohol and hepatocellular carcinoma: a review and a point of view. *World Journal of Gastroenterology: WJG*, *20*(43), 15943. https://doi.org/10.3748/wjg.v20.i43.15943

Thiele, M., Gluud, L. L., Fialla, A. D., Dahl, E. K., & Krag, A. (2014). Large variations in risk of hepatocellular carcinoma and mortality in treatment naïve hepatitis B patients: systematic review with meta-analyses. *Plos One*, *9*(9), e107177. https://doi.org/10.1371/journal.pone.0107177

Tosun, M., Ercisli, S., Ozer, H., Turan, M., Polat, T., Ozturk, E., Padem, H., & Kilicgun, H. (2012). Chemical composition and antioxidant activity of foxtail lily (Eremurus spectabilis). *Acta Scientiarum Polonorum. Hortorum Cultus*, *11*(3).

Tuzcu, Z., Koclar, G., Agca, C. A., Aykutoglu, G., Dervisoglu, G., Tartik, M., & Sahin, K. (2017). Antioxidant, antimicrobial and anticancer effects of different extracts from

wild edible plant Eremurus spectabilis leaves and roots. *International Journal of Clinical and Experimental Medicine*, *10*(3), 4787-4797.

Vidal, I., Torres-Vargas, J. A., Sánchez, J. M., Trigal, M., García-Caballero, M., Medina, M. Á., & Quesada, A. R. (2023). Danthron, an anthraquinone isolated from a marine fungus, is a new inhibitor of angiogenesis exhibiting interesting antitumor and antioxidant properties. *Antioxidants*, *12*(5), 1101. https://doi.org/10.3390/antiox12051101

Vogelstein, B., & Kinzler, K. W. (2004). Cancer genes and the pathways they control. *Nature Medicine*, *10*(8), 789-799.

Wang, C., Cao, Y., Yang, C., Bernards, R., & Qin, W. (2021). Exploring liver cancer biology through functional genetic screens. *Nature Reviews Gastroenterology & Hepatology*, *18*(10), 690-704.

Wang, M.-D., Diao, Y.-K., Yao, L.-Q., Fan, Z.-Q., Wang, K.-C., Wu, H., Gu, L.-H., Xu, J.-H., Li, C., & Lv, G.-Y. (2024). Emerging role of molecular diagnosis and personalized therapy for hepatocellular carcinoma. *Iliver*, 100083. https://doi.org/10.1016/j.iliver.2024.100083

Wang, W., & Wei, C. (2020). Advances in the early diagnosis of hepatocellular carcinoma. *Genes & diseases*, *7*(3), 308-319. https://doi.org/10.1016/j.gendis.2020.01.014

Wang, Y., & Deng, B. (2023). Hepatocellular carcinoma: molecular mechanism, targeted therapy, and biomarkers. *Cancer and Metastasis Reviews*, *42*(3), 629-652.

Weinberg, R. A. (2007). The Biology of Cancer. New York, USA: Garland Science. In: Taylor & Francis Group, LLC.

Wu, H. C., & Santella, R. (2012). The role of aflatoxins in hepatocellular carcinoma. *Hepatitis Monthly*, *12*(10 HCC). https://doi.org/10.5812/hepatmon.7238

Yadav, A. R., & Mohite, S. K. (2020). Cancer-A silent killer: An overview. *Asian Journal of Pharmaceutical Research*, *10*(3), 213-216.

Yang, J. D., Hainaut, P., Gores, G. J., Amadou, A., Plymoth, A., & Roberts, L. R. (2019). A global view of hepatocellular carcinoma: trends, risk, prevention and management. *Nature Reviews Gastroenterology & Hepatology*, *16*(10), 589-604.

Yang, J. D., & Heimbach, J. K. (2020). New advances in the diagnosis and management of hepatocellular carcinoma. *Bmj*, *371*. https://doi.org/10.1136/bmj.m3544

Yao, C., Wu, S., Kong, J., Sun, Y., Bai, Y., Zhu, R., Li, Z., Sun, W., & Zheng, L. (2023). Angiogenesis in hepatocellular carcinoma: mechanisms and anti-angiogenic

therapies. *Cancer Biology & Medicine*, *20*(1), 25. https://doi.org/10.20892/j.issn.2095-3941.2022.0449

Yoshiji, H., Kuriyama, S., Hicklin, D. J., Huber, J., Yoshii, J., Miyamoto, Y., Kawata, M., Ikenaka, Y., Nakatani, T., & Tsujinoue, H. (1999). KDR/Flk-1 is a major regulator of vascular endothelial growth factor-induced tumor development and angiogenesis in murine hepatocellular carcinoma cells. *Hepatology*, *30*(5), 1179-1186. https://doi.org/10.1002/hep.510300509

Zhang, X., Shao, J., Li, X., Cui, L., & Tan, Z. (2019). Docetaxel promotes cell apoptosis and decreases SOX2 expression in CD133-expressing hepatocellular carcinoma stem cells by suppressing the PI3K/AKT signaling pathway. *Oncology Reports*, *41*(2), 1067-1074. https://doi.org/10.3892/or.2018.6891

Zhu, D., Tao, W., Zhang, H., Liu, G., Wang, T., Zhang, L., Zeng, X., & Mei, L. (2016). Docetaxel (DTX)-loaded polydopamine-modified TPGS-PLA nanoparticles as a targeted drug delivery system for the treatment of liver cancer. *Acta Biomaterialia*, *30*, 144-154. https://doi.org/10.1016/j.actbio.2015.11.031

Zhu, R. X., Seto, W.-K., Lai, C.-L., & Yuen, M.-F. (2016). Epidemiology of hepatocellular carcinoma in the Asia-Pacific region. *Gut and liver*, *10*(3), 332. https://doi.org/10.5009/gnl15257